

# Optical absorption in boron clusters $B_6$ and $B_6^+$ : a first principles configuration interaction singles approach\*

Ravindra Shinde<sup>a</sup> and Alok Shukla

Department of Physics, Indian Institute of Technology Bombay, 400076 Mumbai, Maharashtra, India

Received 31 August 2012 / Received in final form 27 February 2013

Published online 7 May 2013 – © EDP Sciences, Società Italiana di Fisica, Springer-Verlag 2013

**Abstract.** The linear optical absorption spectra in neutral boron cluster  $B_6$  and cationic  $B_6^+$  are calculated using a first principles correlated electron approach. The geometries of several low-lying isomers of these clusters were optimized at the coupled-cluster singles doubles (CCSD) level of theory. With these optimized ground-state geometries, excited states of different isomers were computed using the configuration-interaction singles (CIS) approach. The many-body wavefunctions of various excited states have been analyzed and the nature of optical excitation involved are found to be of collective, plasmonic type. We also benchmark our CIS results against more sophisticated equation-of-motion (EOM) CCSD approach for a few isomers.

## 1 Introduction

The cluster science is now a fast emerging field due to the discovery of novel properties of clusters with tremendous potential for applications. A cluster of atoms, or molecules can have few atoms to thousands of atoms in it, with various structural forms, such as spheres, tubes, planar structures, etc. Most of the time, the properties exhibited by clusters are quite different as compared to their bulk counterpart [1,2]. Boron, in particular, is as interesting as carbon, because of its short covalent radius and ability to form any structure due to catenation [3]. Boron also exhibits structures like nanotubes, fullerenes, planar sheets, etc. [4–6]. Some of the structures of boron have been studied in the context of hydrogen storage [7]. Both  $\sigma$  and  $\pi$  aromaticity is observed in many planar boron clusters. Some planar boron structures are also found to be analogous to hydrocarbons [8]. A circular  $B_{19}^-$  cluster, with a unit of  $B_6$  wheel in the center behaves as a Wankel motor, i.e. the inner  $B_6$  wheel rotating opposite to the outer  $B_{13}$  ring [9,10]. The all-boron clusters are promising candidates as inorganic ligands [11,12].

There have been various experimental and theoretical investigations of bare boron clusters. Electronic structures of boron quasi-planar structures, tubes, wheels and rings were studied experimentally using photo-emission spectroscopy by Kiran et al. [4], Romanescu et al. [5], and Zhai et al. [6,8]. They also gave a density functional theory (DFT) based explanation of their electronic structure. Alexandrova et al. [13] explored the structural and

electronic properties and chemical bonding in  $B_6^-$  and  $B_6$  using anion photoelectron spectroscopy and ab initio calculations. Placa et al. [14] studied abundance spectrum of boron clusters generated using laser ablation technique. Ionic boron clusters were experimentally studied by Hanley et al. [15]. They studied the fragmentation of bigger clusters into smaller ones by studying the collision-induced dissociation of boron clusters. Boustani, on the other hand, gave a theoretical description of electronic structures of small bare boron clusters using configuration interaction method, although with a relatively small Gaussian basis set [16]. Recently, a DFT based study of bare boron clusters was done by Atiş et al. [17]. As far as optical properties of boron clusters are concerned, only a small number of reports available. Botti et al. [18] studied the optical absorption spectra of  $B_{20}$ ,  $B_{38}$ ,  $B_{44}$ ,  $B_{80}$  and  $B_{92}$  using time-dependent DFT. To the best of our knowledge, no other experimental results are available on the optical absorption of boron clusters.

Our group has recently studied the optical absorption in boron clusters  $B_n$  ( $n = 2-5$ ) using a large-scale multi-reference configuration interaction method [19]. Since this method is quite expensive and scales as  $N^6$ , where  $N$  is the number of orbitals used in the calculations, it becomes more and more computationally demanding for large clusters, or clusters with no symmetry. However, good insights can be achieved with much less expensive method known as configuration interaction singles (CIS), containing only one electron excitations from the Hartree-Fock ground state [20]. This method has been extensively used for the study of the excited states and optical absorption in various other systems [21–26]. Since optical absorption spectra is very sensitive to the structural geometry, the optical absorption spectroscopy along with the extensive calculations of optical absorption spectra, can be used to

\* ISSPIC 16 - 16th International Symposium on Small Particles and Inorganic Clusters, edited by Kristiaan Temst, Margriet J. Van Bael, Ewald Janssens, H.-G. Boyen and Françoise Remacle.

<sup>a</sup> e-mail: ravindra.shinde@iitb.ac.in

distinguish between distinct isomers of a cluster. In this report, we present extensive calculations of the linear optical absorption spectrum of low-lying isomers of  $B_6$  and  $B_6^+$  clusters with different structures. This study, along with the experimental absorption spectra, can lead to identification of these distinct isomers. Also, in the interpretation of the measured spectra, the theoretical understanding of the excited states of clusters plays an important role [27].

The remainder of this paper is organized as follows. Next section describes the theoretical and computational details of the work, followed by Section 3, in which results are presented and discussed. In the last section, we present our conclusions, and explore the scope for future work. Detailed information regarding the excited states contributing to the optical absorption is presented in the Appendix.

## 2 Theoretical and computational details

Different possible arrangements and orientations of atoms of the  $B_6$  cluster (both neutral and cationic) were randomly selected for the initial configurational search of geometries of isomers. For a given spin multiplicity, the geometry optimization was done at a correlated level, i.e., at the singles doubles coupled cluster (CCSD) level [28] with 6-311G(d,p) basis set as implemented in GAUSSIAN 09 [29]. Since neutral cluster can have singlet or higher spin multiplicity, the optimization was repeated for different spin configurations to get the lowest energy isomer. Similarly for cationic clusters with odd number of electrons, spin multiplicities of 2 and 4 were considered in the optimization. In total, we have obtained 11 neutral  $B_6$  and 8 cationic  $B_6^+$  low-lying isomers. These optimized geometries of neutral  $B_6$  cluster, as shown in Figure 1, are found to be in good agreement with other available reports. Figure 15 shows the corresponding geometries of cationic  $B_6^+$  cluster. The unique bond lengths, point group symmetry and the electronic ground states are given in respective sub-figures.

The excited state energies of isomers are obtained using the ab initio CIS approach. In this method, different configurations are constructed by promoting an electron from an occupied orbital to a virtual orbital. For open-shell systems, we have used unrestricted Hartree-Fock formalism for constructing CIS configurations. Excited states of the system will have a linear combination of all such substituted configurations, with corresponding variational coefficients. The energies of the excited states will then be obtained by diagonalizing the Hamiltonian in this configurational space<sup>1</sup>. The dipole matrix elements are calculated using the ground state and the excited state wavefunctions. This is subsequently used for calculating the optical absorption cross section assuming Lorentzian lineshape, with some artificial finite linewidth.

<sup>1</sup> L.E. McMurchie, S.T. Elbert, S.R. Langhoff, E.R. Davidson, MELD package from Indiana University. It has been modified by us to handle bigger systems.

Equation-of-motion CCSD (EOM-CCSD) calculations were done on few representative clusters in order to justify the use of single-excitation CIS method for optical absorption calculations [30,31]. Details are discussed in the next section. The contribution of wavefunction of the excited states to the absorption peaks as well as an analysis based on natural transition orbitals gives an insight into the nature of optical excitation.

In one of the earlier reports published elsewhere [19], we have extensively studied the dependence of basis sets, freezing of  $1s^2$  chemical core on the computed photoabsorption spectra of neutral boron clusters [19]. We have shown that the optical absorption spectra of small boron clusters do not change even if we freeze the chemical core of boron atoms. Therefore, in all these calculations  $1s^2$  chemical core of each boron atom has been frozen.

## 3 Results and discussion

In this section, we discuss the structure and energetics of various isomers of neutral and cationic  $B_6$  cluster, followed by discussion of results of computed absorption spectra and nature of photo-excitations.

In the many-particle wavefunction analysis of excited states contributing to the various peaks, we have used following convention. For doublet systems  $H_{1\alpha}$  denotes the singly occupied molecular orbital. For triplet systems, two singly occupied molecular orbitals (SOMO) are denoted by  $H_{1\alpha}$  and  $H_{2\alpha}$ , while  $H$  and  $L$  stands for highest occupied molecular orbital and lowest unoccupied molecular orbital, respectively. For quartets, the third singly occupied molecular orbital is denoted by  $H_{3\alpha}$ .

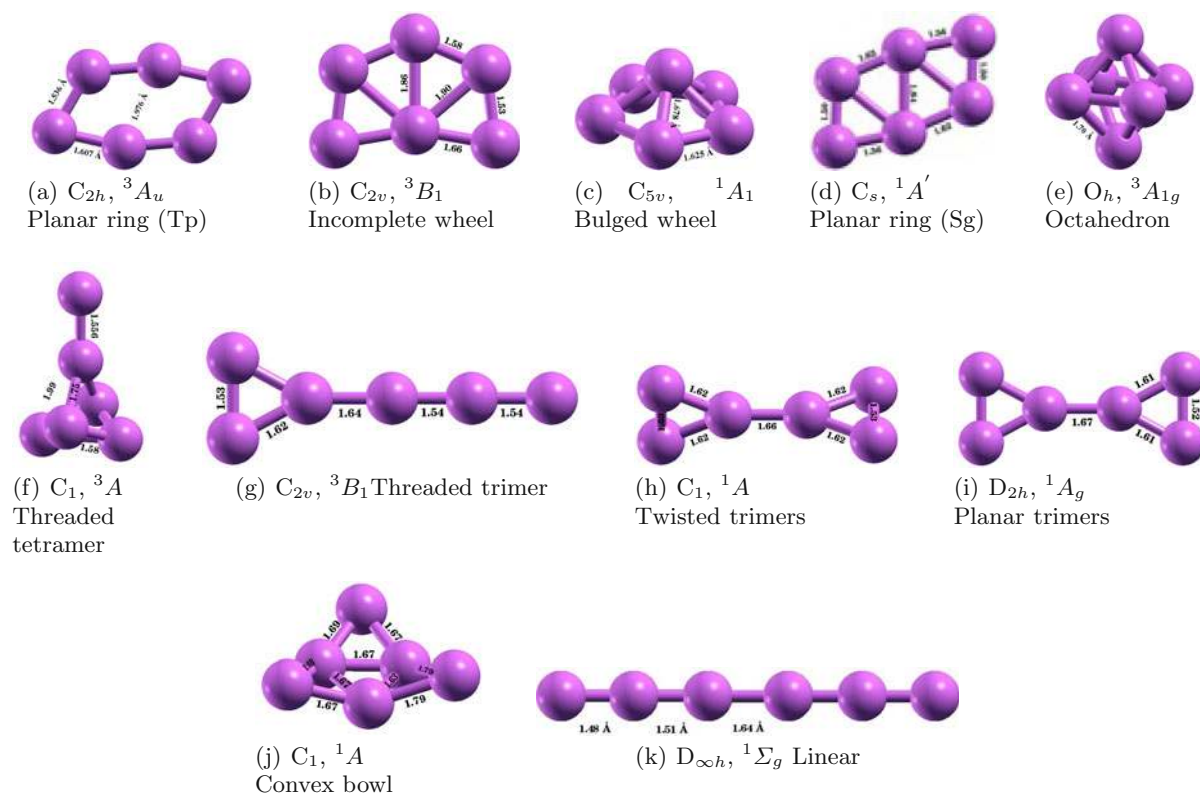
### 3.1 $B_6$

We have found a total of 11 isomers of neutral  $B_6$  cluster with stable geometries as shown in Figure 1 [32]. The relative standings in energy are presented in the Table 1, along with point group symmetries and electronic states.

The most stable isomer of  $B_6$  cluster has ring-like planar structure, with  $C_{2h}$  point group symmetry. Although  $B_6$  has an even number of electrons, the electronic ground state of this isomer is a triplet – an open shell system. The equilibrium geometry obtained in our calculation is in good agreement with the recently reported values [13,17,33,34]. The optical absorption spectrum calculated using the CIS approach is as shown in Figure 2. It is mainly characterized by feeble absorption in the visible range, but much stronger absorption at higher energies. The many particle wavefunctions of excited states contributing to various peaks are presented in Table A.1. The first absorption peak at 2.85 eV with very low intensity is characterized by  $H_\alpha - 2 \rightarrow L_\alpha$  and  $H_{1\alpha} \rightarrow L_\alpha$  transitions. The natural transition orbital analysis of the peak at 3.42 eV shows that this is dominated by a  $\pi \rightarrow \pi^*$  transition. Due to planar nature of the isomer, we can classify the absorption into two categories: (a) those with polarization along the direction of the plane and (b) polarization

**Table 1.** Point group, electronic state, total energies and values of  $\langle S^2 \rangle$  before and after ( $\langle S_a^2 \rangle$ ) spin annihilation operation for different isomers of  $B_6$  cluster.

Sr. No.	Isomer	Point group	Elect. state	Total energy (Ha)	$\langle S^2 \rangle$	$\langle S_a^2 \rangle$
1	Planar ring (triplet)	$C_{2h}$	$^3A_u$	-147.795051	2.720	2.180
2	Incomplete wheel	$C_{2v}$	$^3B_1$	-147.774166	2.750	2.217
3	Bulged wheel	$C_{5v}$	$^1A_1$	-147.764477	0.000	0.000
4	Planar ring (singlet)	$C_s$	$^1A'$	-147.720277	0.000	0.000
5	Octahedron	$O_h$	$^3A_{1g}$	-147.678302	2.082	2.003
6	Threaded tetramer	$C_1$	$^3A$	-147.676776	2.019	2.000
7	Threaded trimer	$C_{2v}$	$^3B_1$	-147.667709	2.087	2.001
8	Twisted trimers	$C_1$	$^1A$	-147.645847	0.000	0.000
9	Planar trimers	$D_{2h}$	$^1A_g$	-147.645522	0.000	0.000
10	Convex bowl	$C_1$	$^1A$	-147.612607	0.000	0.000
11	Linear	$D_{\infty h}$	$^1\Sigma_g$	-147.449013	0.000	0.000

**Fig. 1.** Geometry optimized ground state structures of different isomers of neutral  $B_6$  clusters, along with the point group symmetries obtained at the CCSD level.

perpendicular to the plane. In this case, it is seen that, in most of the cases, the absorption is due to polarizations along the plane of the isomer. Also, instead of being dominated by single configurations, the wavefunctions of the excited states contributing to all the peaks exhibit strong configuration mixing. This is an indicator of plasmonic nature of the optical excitations [35].

The optical absorption spectrum for the same isomer is calculated using a sophisticated EOM-CCSD method,

as shown in Figure 3. A complete one-to-one mapping of configurations involved in excited states of CIS and EOM-CCSD calculations is observed, along with some double excitations with minor contribution. The spectrum of EOM-CCSD is red-shifted, as expected, because this method takes electron correlations into account at a high level.

The second low lying isomer of  $B_6$  is another planar structure resembling an incomplete wheel, i.e. one outer

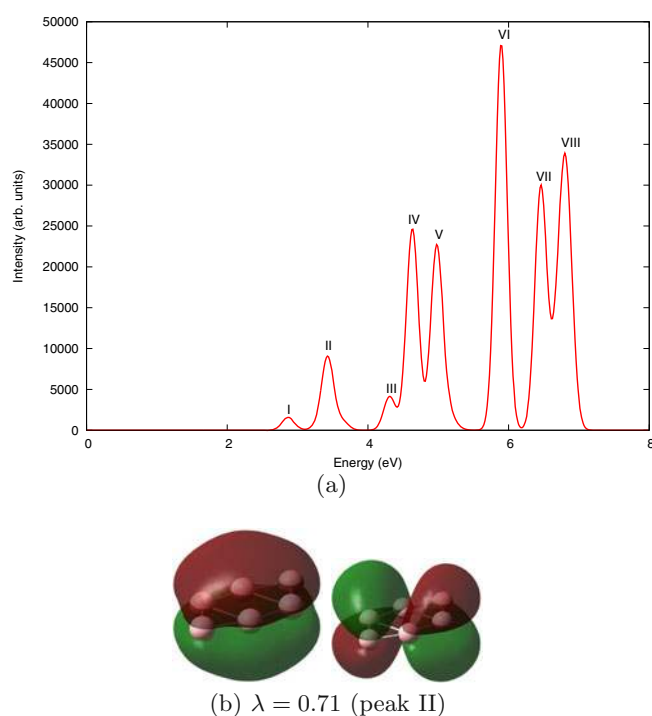


**Fig. 2.** The linear optical absorption spectrum of planar ring (triplet)  $B_6$  isomer, calculated using the CIS approach, along with the natural transition orbitals involved in the excited states corresponding to the peak II (3.42 eV). Parameter  $\lambda$  refers to a fraction of the NTO pair contribution to a given electronic excitation.

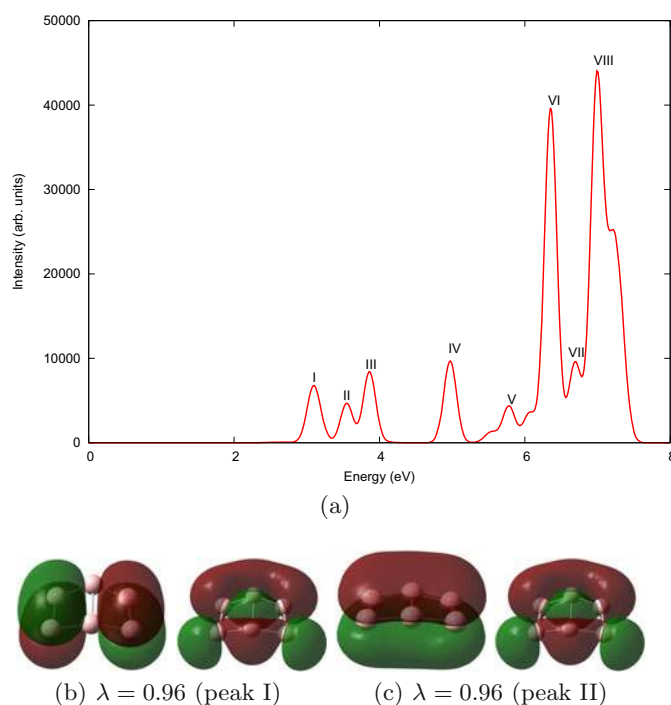


**Fig. 4.** The linear optical absorption spectrum of incomplete-wheel  $B_6$  isomer, calculated using the CIS approach, along with the natural transition orbitals involved in the excited states corresponding to the peaks I (3.09 eV) and II (3.55 eV), respectively. Parameter  $\lambda$  refers to a fraction of the NTO pair contribution to a given electronic excitation.

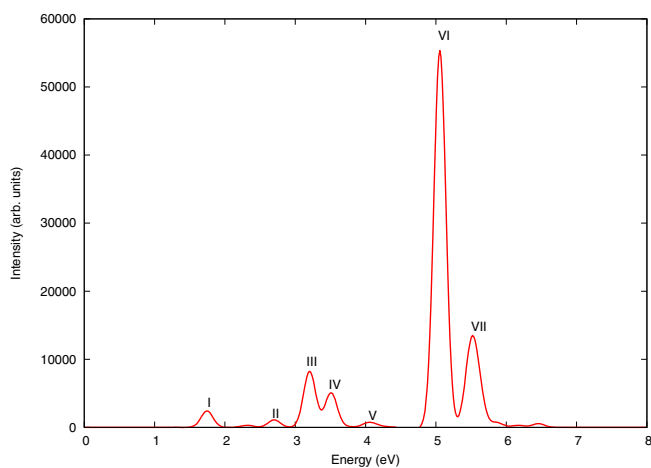


**Fig. 3.** The linear optical absorption spectrum of planar ring (triplet)  $B_6$  isomer, calculated using the EOM-CCSD approach.

atom removed from  $B_7$  wheel cluster. This isomer is also a triplet system with  $C_{2v}$  symmetry, lying 0.56 eV above the global minimum structure. The optimized geometry is in good agreement with the other previously available reports [33,36]. This is one of the isomers showing feeble optical absorption at lower energies (cf. Fig. 4). The many particle wavefunctions of excited states contributing

to various peaks are presented in Table A.3. Degenerate  $\pi$  orbitals are involved in the excitations at peak I and II as evident from the NTOs shown in Figure 4.

A wheel kind of structure, with its center slightly bulged out, is found to be the next stable isomer of  $B_6$ . A singlet system with  $C_{5v}$  point group symmetry, lies just 0.83 eV above in energy as compared to the most stable isomer. The pentagonal base has bond length of 1.625 Å and the vertex atom is 1.678 Å apart from the corners of the pentagon. Other reported values for those bond lengths are 1.61 Å, 1.66 Å [17,36] and 1.61 Å, 1.659 Å [13,33], respectively. The optical absorption spectrum calculated using CIS approach is presented in Figure 5. The many-particle wavefunctions of excited states contributing to various peaks are presented in Table A.4. The onset of the spectrum occurs near 3.76 eV, with polarization in the plane of the pentagonal base, characterized by excitations  $H - 1 \rightarrow L + 6$  and  $H \rightarrow L + 6$  with equal contribution.

The spectrum of this singlet isomer is calculated again using EOM-CCSD approach to investigate any involvement of double excitation. The spectrum appears to be red-shifted but the configurations contributing to the excited states corresponding to the peaks of the spectrum are the same as observed in the case of CIS (Fig. 6). This makes us confident to use CIS method only to investigate optical absorption spectrum of other isomers.

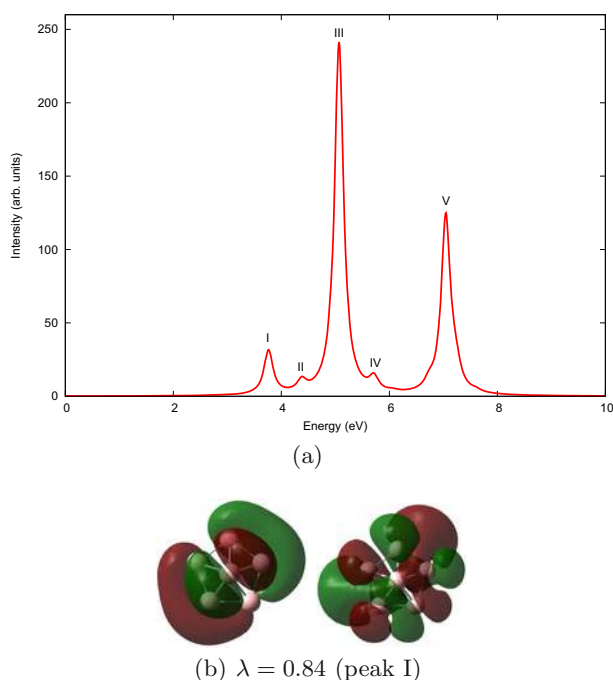


**Fig. 5.** The linear optical absorption spectrum of bulged-wheel  $B_6$  isomer, calculated using the CIS approach, along with the natural transition orbitals involved in the excited states corresponding to the peak I (3.76 eV). Parameter  $\lambda$  refers to a fraction of the NTO pair contribution to a given electronic excitation.

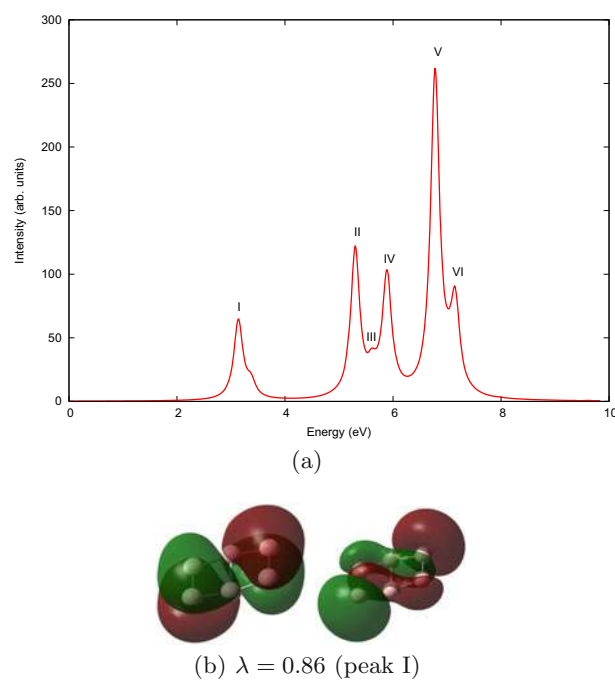


**Fig. 7.** The linear optical absorption spectrum of planar-ring  $B_6$  isomer, calculated using the CIS approach, along with the natural transition orbitals involved in the excited states corresponding to the peak I (3.13 eV). Parameter  $\lambda$  refers to a fraction of the NTO pair contribution to a given electronic excitation.

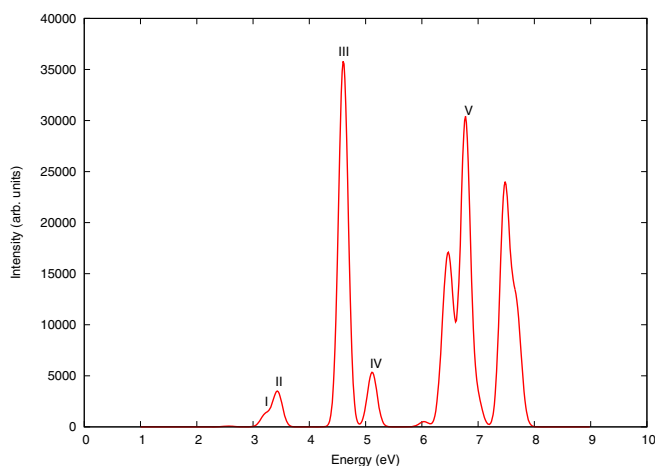


**Fig. 6.** The linear optical absorption spectrum of bulged-wheel  $B_6$  isomer, calculated using the EOM-CCSD approach.

A planar ring like structure, resembling the global minimum one; however, with singlet state and  $C_s$  symmetry, is the next low lying isomer of  $B_6$  cluster. The optimized geometry is in good agreement with reference [36]. The absorption spectrum is presented in Figure 7 and corresponding many-particle wavefunctions of various excited states are presented in Table A.6. The absorption onset occurs at 3.1 eV, characterized by delocalized orbitals with  $H - 1 \rightarrow L$  and  $H \rightarrow L + 23$  configurations.

An octahedron structure with  $O_h$  point group symmetry is the next stable isomer of neutral  $B_6$ . Each side of the octahedron is found to be 1.7 Å as compared to the 1.68 Å reported by references [17,36]. The many-particle wavefunctions of the excited states corresponding to various peaks (cf. Fig. 8) are presented in Table A.7. A very feeble absorption at 0.92 eV opens the spectrum, mainly characterized by excitations  $H_{1\alpha} \rightarrow L_\alpha$  and  $H_{2\alpha} \rightarrow L_\alpha + 1$  with equal contribution. The transition orbitals corresponding to peaks at 0.92 eV and 2.50 eV are as shown in Figure 8.

Next isomer is previously unreported, with structure of a saddle threaded with dimer from top. It lies just 0.04 eV above the previous octahedron isomer. However, the optical absorption spectrum (cf. Fig. 9) is completely different. A narrow energy range hosts all the peaks. The onset of spectrum occurs near 3.06 eV, with major contribution from  $H_{2\alpha} \rightarrow L_\alpha + 2$  (cf. Tab. A.8). The NTO analysis shows that excitation occurs from the tail end to the saddle section of the isomer.

An isosceles triangle connected to a linear chain of boron atoms forms the next isomer. This structure with  $C_{2v}$  symmetry and a triplet electronic state have been reported in reference [36], which is in close agreement with our results. The optical absorption spectrum (cf. Fig. 10) has distinctive closely lying peaks at 4.03 eV and 4.73 eV. The many-particle wavefunctions of excited states corresponding to various peaks are presented in Table A.9. As evident from the NTOs involved in transitions at peak I,

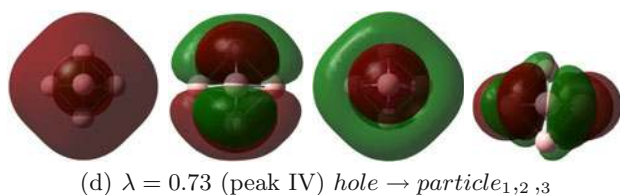
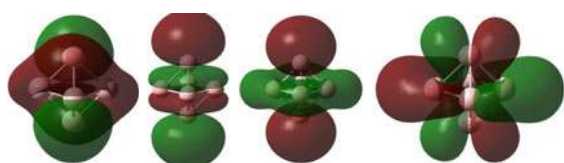
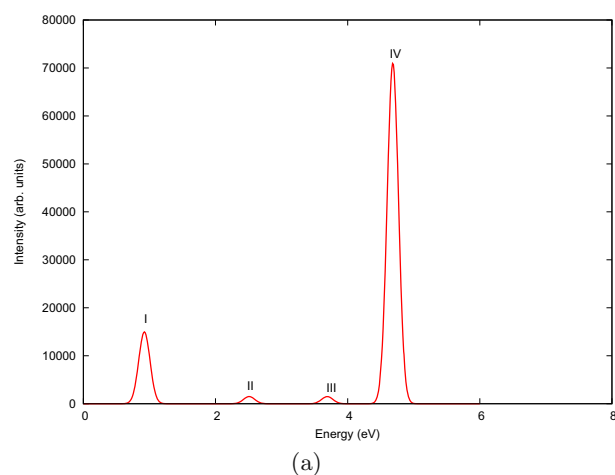
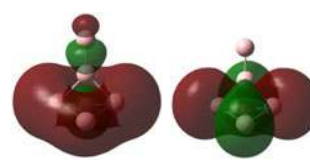
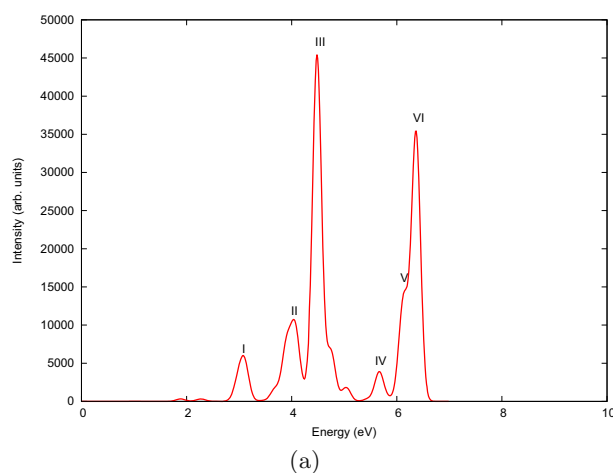


**Fig. 8.** The linear optical absorption spectrum of octahedron  $B_6$  isomer, calculated using the CIS approach, along with the natural transition orbitals involved in the excited states corresponding to the peaks I (0.92 eV) and IV (4.68 eV), respectively. Parameter  $\lambda$  refers to a fraction of the NTO pair contribution to a given electronic excitation.

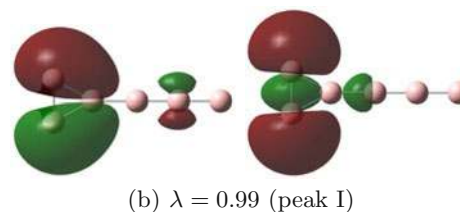
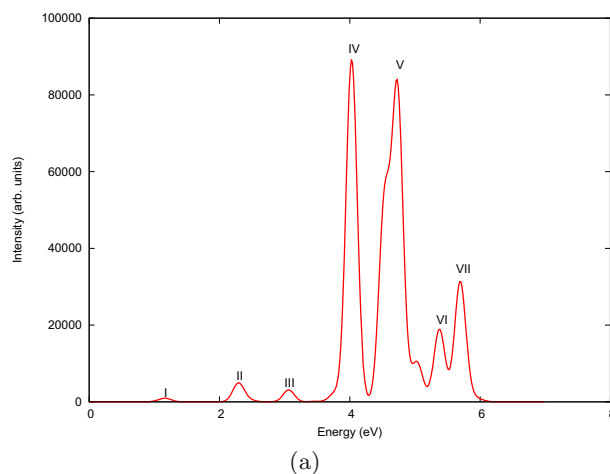
the electrons tend to be localized at the triangular end of the isomer.

A structure with two out of plane isosceles triangles joined together is found to be one of the isomers. The geometry has isosceles triangle with lengths 1.62 Å, 1.62 Å and 1.53 Å, while two such triangles are joined by a bond of length 1.66 Å. The respective numbers reported by reference [36] are 1.60 Å, 1.60 Å, 1.50 Å and 1.647 Å, respectively. The optical absorption spectrum contains many low intensity peaks except for strongest one at 5.87 eV, as presented in Figure 11. A  $\pi \rightarrow \pi^*$  transition is observed at 2.22 eV. (cf. Tab. A.10).

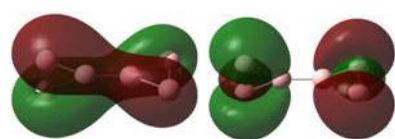
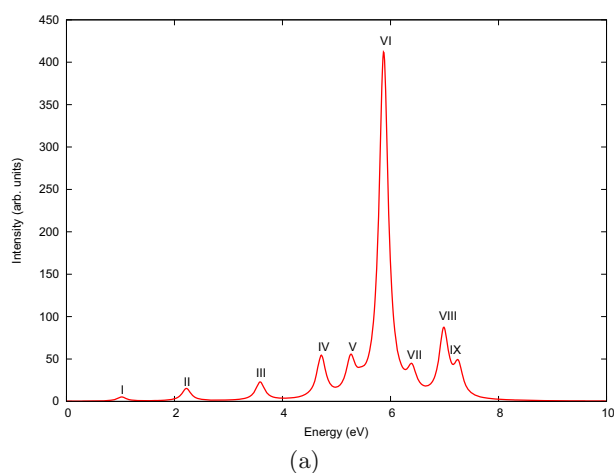
An almost degenerate structure forms the next isomer, lying just 0.009 eV above the previous isomer. Contrary to the previous one, this geometry is completely planar and is a triplet system, with  $C_{2v}$  point group symmetry. Probably because of such a strong near-degeneracy, this isomer has not been reported in the literature before. The many-particle wavefunctions of the excited states corresponding to various peaks (cf. Fig. 12) are presented in Table A.11. The spectrum opens with feeble peak. First major peak



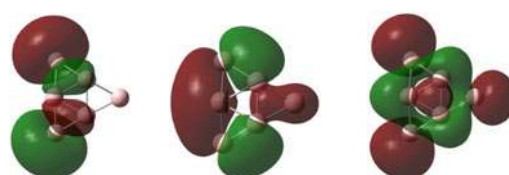
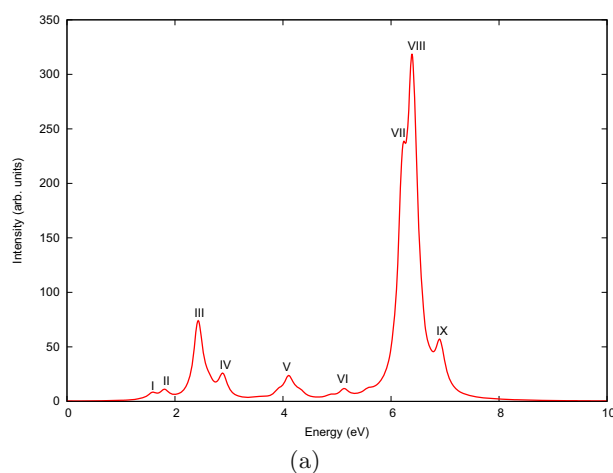
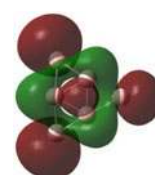
**Fig. 9.** The linear optical absorption spectrum of threaded-tetramer  $B_6$  isomer, calculated using the CIS approach, along with the natural transition orbitals involved in the excited states corresponding to the peak I (3.06 eV). Parameter  $\lambda$  refers to a fraction of the NTO pair contribution to a given electronic excitation.



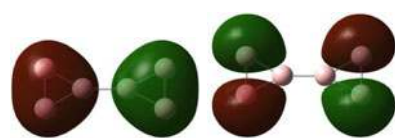
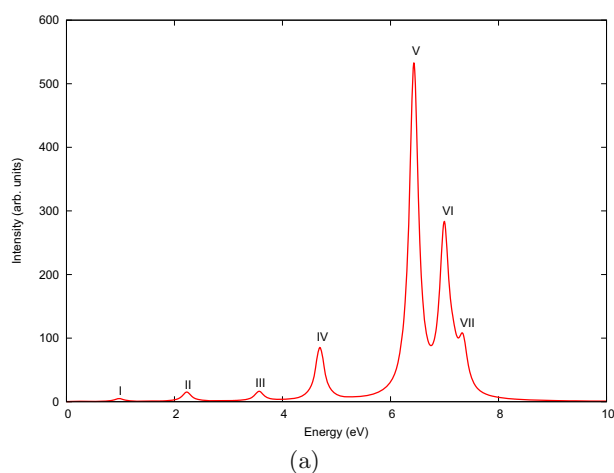
**Fig. 10.** The linear optical absorption spectrum of threaded-trimer  $B_6$  isomer, calculated using the CIS approach, along with the natural transition orbitals involved in the excited states corresponding to the peak II (2.28 eV). Parameter  $\lambda$  refers to a fraction of the NTO pair contribution to a given electronic excitation.

(b)  $\lambda = 0.63$  (peak I)

**Fig. 11.** The linear optical absorption spectrum of twisted trimers  $B_6$  isomer, calculated using the CIS approach, along with the natural transition orbitals involved in the excited states corresponding to the peak II (2.22 eV). Parameter  $\lambda$  refers to a fraction of the NTO pair contribution to a given electronic excitation.

(b)  $\lambda = 0.76$  (peak III)(c)  $\lambda = 0.22$  (peak IV)

**Fig. 13.** The linear optical absorption spectrum of convex-bowl  $B_6$  isomer, calculated using the CIS approach, along with the natural transition orbitals involved in the excited states corresponding to the peaks III (2.43 eV) and IV (2.88 eV), respectively. Parameter  $\lambda$  refers to a fraction of the NTO pair contribution to a given electronic excitation.

(b)  $\lambda = 0.22$  (peak IV)

**Fig. 12.** The linear optical absorption spectrum of planar trimers  $B_6$  isomer, calculated using the CIS approach, along with the natural transition orbitals involved in the excited states corresponding to the peak IV (4.69 eV). Parameter  $\lambda$  refers to a fraction of the NTO pair contribution to a given electronic excitation.

at 4.69 eV is characterized by  $\pi \rightarrow \pi^*$  transition, as is evident from the natural transition orbital analysis. First four peaks in the absorption spectra of this isomer are identical to that of twisted trimers isomer. The effect of twisting has effect only on the high energy excitations.

Convex bowl shaped isomer and a perfect linear chain are found very high in energy, ruling out their existence at room temperature. The optical spectra are presented in Figures 13 and 14, respectively. The corresponding many-particle wavefunctions of excited states of various peaks are presented in Tables A.12 and A.13. Peak at 2.43 eV in the absorption spectrum of convex bowl isomer shows partially delocalized to fully delocalized nature of transition. The bulk of the oscillator strength of the spectrum of linear isomer is carried by  $H - 1 \rightarrow L + 3$  and  $H \rightarrow L + 2$  having equal contributions. The NTOs corresponding to the excitations involved in the spectrum are shown in Figure 14.

### 3.2 $B_6^+$

We have found a total of 8 isomers of cationic ( $B_6^+$ ) cluster with stable geometries as shown in Figure 15. The relative standings in energy are presented in Table 2, along with point group symmetries, electronic states and expectation

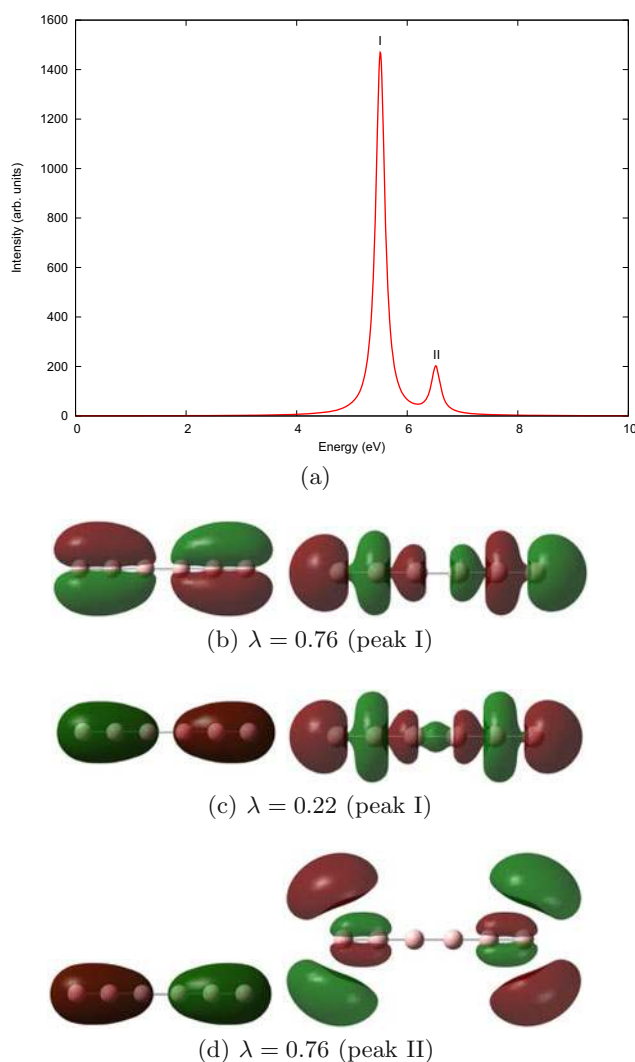


**Fig. 14.** The linear optical absorption spectrum of linear B<sub>6</sub> isomer, calculated using the CIS approach, along with the natural transition orbitals involved in the excited states corresponding to the peaks I (5.51 eV) and II (6.51 eV), respectively. Parameter  $\lambda$  refers to a fraction of the NTO pair contribution to a given electronic excitation.

value of  $S^2$  operator. Since this is a case of an open-shell system, the spin contamination may induce large errors in the computed absorption spectra. We have reported  $\langle S^2 \rangle$  values for excited states corresponding to each peak in the spectra. In most of the cases the geometry of the neutral isomer is retained, reflected in the fact that some peaks show up in the optical absorption spectra at the same energies as those in the neutral cluster.

The most stable isomer of B<sub>6</sub><sup>+</sup> cluster is a planar ring-type of structure, with C<sub>s</sub> point group symmetry. This is in contrast to the other reported geometries which have D<sub>2h</sub> symmetry [33,34,36]. A slight difference in the orientation makes it less symmetric. However, the bonds lengths obtained are in good agreement with those with D<sub>2h</sub> symmetric geometry cited above. The optical

absorption spectrum calculated using CIS approach is as shown in Figure 16 and corresponding many-particle wavefunctions of excited states contributing to the various peaks are presented in Table A.14. Similar to the neutral counterpart, this isomer also has very feeble absorption in the visible range, with polarization perpendicular to the plane of the isomer. Transitions involved corresponding to peak 4.44 eV are from completely delocalized orbitals to the localized ones on each corner of the isomer.

Bulged wheel structure is the next low lying isomer of B<sub>6</sub><sup>+</sup> with just 0.023 eV above the global minimum. However, as compared to the neutral one, this geometry has C<sub>1</sub> symmetry due to the significant bond length reordering. Our computed geometries are consistent with the results of references [33,36]. The optical absorption spectrum is presented in Figure 17. The many-particle wavefunctions of excited states contributing to various peaks are presented in Table A.15. The spectrum is distinctly different with a large number of smaller peaks and a stronger peak at 6.24 eV. The onset of spectrum occurs at 1.76 eV dominated by  $H_\beta \rightarrow L_\beta$  and  $H_{\beta-1} \rightarrow L_\beta$  configurations.

Another ring-like structure with D<sub>2h</sub> symmetry and doublet multiplicity lies next in the energy order. The hexagonal benzene type structure has 1.66 Å and 1.53 Å as unique bond lengths, which are somewhat larger than those reported in references [33,36]. The optical absorption spectrum presented in Figure 18, is fairly simple and has well resolved peaks. The many-particle wavefunctions of excited states contributing to various peaks are presented in Table A.16. All absorption peaks are due to the polarization along the plane of the isomer. The strongest absorption is seen at 3.52 eV with fully delocalized to partially localized nature of transition.

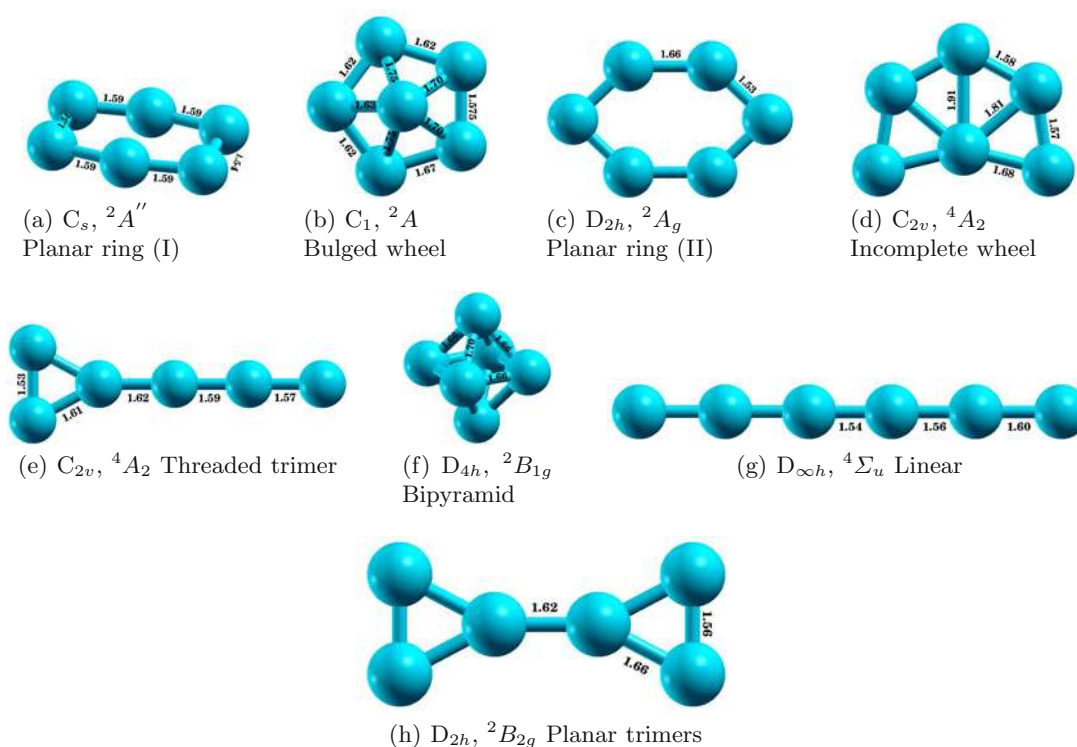
Next low lying isomer is a planar incomplete wheel structure with C<sub>2v</sub> point group symmetry and quartet multiplicity. This multiplicity and computed geometry is consistent with results of reference [36]. The optical absorption (cf. Fig. 19) starts at 1.69 eV, with polarization transverse to the plane of the isomer. The many particle wavefunctions of excited states contributing to various peaks are presented in Table A.17. The configurations contributing to the first peak are  $H_\beta - 2 \rightarrow L_\beta$ .

Another isomer with the same point group symmetry and multiplicity as that of the previous one, but having a geometry of linear chain with an isosceles triangle at the end, is the next low lying isomer of cationic B<sub>6</sub><sup>+</sup>. Our results about geometry are in good agreement with the reference [36]. The optical absorption spectrum (cf. Fig. 20) has very few major peaks. The first major peak occurs at 3.90 eV, with polarization along the plane of the isomer, and has dominant contribution from  $H_{3\alpha} \rightarrow L_\alpha + 1$  (cf. Tab. A.18).

Tetragonal bipyramid forms the next stable isomer of cationic B<sub>6</sub><sup>+</sup>, with D<sub>4h</sub> point group symmetry and doublet multiplicity. This is in good agreement with the geometries reported in references [33,36]. The optical absorption spectrum (cf. Fig. 21) has well defined small number of peaks.  $H_{1\alpha} \rightarrow L_\alpha$  and  $H_\alpha - 4 \rightarrow L_\alpha$  contributes dominantly to

**Table 2.** Point group, electronic state, total energies and values of  $\langle S^2 \rangle$  before and after spin annihilation operation for different isomers of  $B_6^+$  cluster.

Sr. No.	Isomer	Point group	Elect. state	Total energy (Ha)	$\langle S^2 \rangle$	$\langle S_a^2 \rangle$
1	Planar ring (I)	$C_s$	$^2A''$	-147.492831	0.8410	0.7524
2	Bulged wheel	$C_1$	$^2A$	-147.491994	1.0450	0.7909
3	Planar ring (II)	$D_{2h}$	$^2A_g$	-147.480796	0.8503	0.7531
4	Incomplete wheel	$C_{2v}$	$^4A_2$	-147.454234	4.6090	3.9490
5	Threaded trimer	$C_{2v}$	$^4A_2$	-147.429627	3.7671	3.7501
6	Tetra. bipyramid	$D_{4h}$	$^2B_{1g}$	-147.413145	1.2565	0.8742
7	Linear	$D_{\infty h}$	$^4\Sigma_u$	-147.392263	4.8354	4.0712
8	Planar trimers	$D_{2h}$	$^2B_{2g}$	-147.358494	1.0000	0.7808

**Fig. 15.** Geometry optimized ground state structures of different isomers of cationic  $B_6^+$  clusters, along with the point group symmetries obtained at the CCSD level.

peaks in the visible range at 1.23 eV and 2.55 eV, respectively (cf. Tab. A.19).

Two more structures were found stable, i.e., (a) a planar structure with two trimers joined together and, (b) a linear one. These isomers are much above the global minimum energy, it rules out their room temperature existence. In the linear isomer the absorption spectrum (cf. Fig. 22) is red-shifted as compared to the neutral one, with major peak at 4.25 eV with dominant contribution from  $H_\beta - 1 \rightarrow L_\beta + 1$  and  $H_\beta \rightarrow L_\beta$  configurations. In case of planar trimers structure, the spectrum (cf. Fig. 23) also seems to be red shifted as compared to the neutral one. The first peak is found at 1.40 eV with  $H_\beta \rightarrow L_\beta$  and

$H_\beta - 2 \rightarrow L_\beta + 1$ , characterized by  $\pi \rightarrow \pi^*$  transition, as dominant contribution to the wavefunction of the excited state.

## 4 Conclusion and outlook

A large number of randomly selected initial structures of neutral  $B_6$  and cationic  $B_6^+$  clusters are taken into consideration for locating the global and local minimas on the potential energy curves. A careful geometry optimization is done for all those structures at a correlated level. The optical absorption spectra of different low-lying isomers

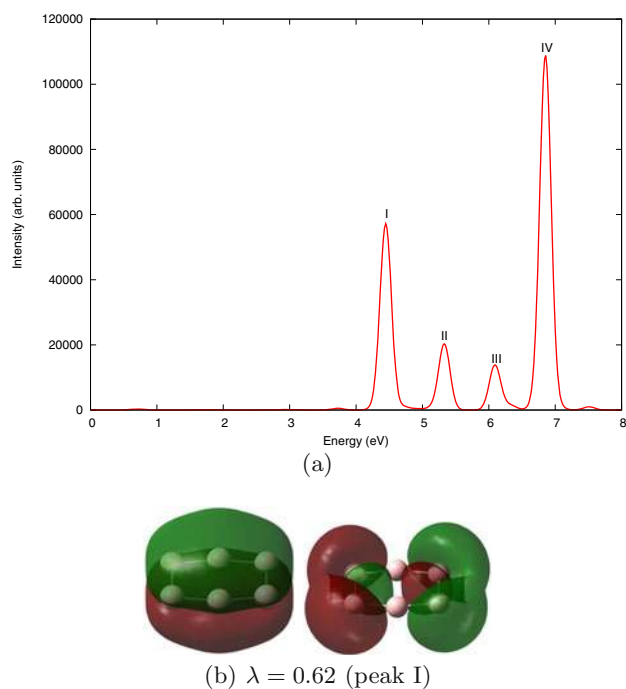


**Fig. 16.** The linear optical absorption spectrum of planar ring  $B_6^+$  isomer (I), calculated using the CIS approach, along with the natural transition orbitals involved in the excited states corresponding to the peak I (4.44 eV). Parameter  $\lambda$  refers to a fraction of the NTO pair contribution to a given electronic excitation.

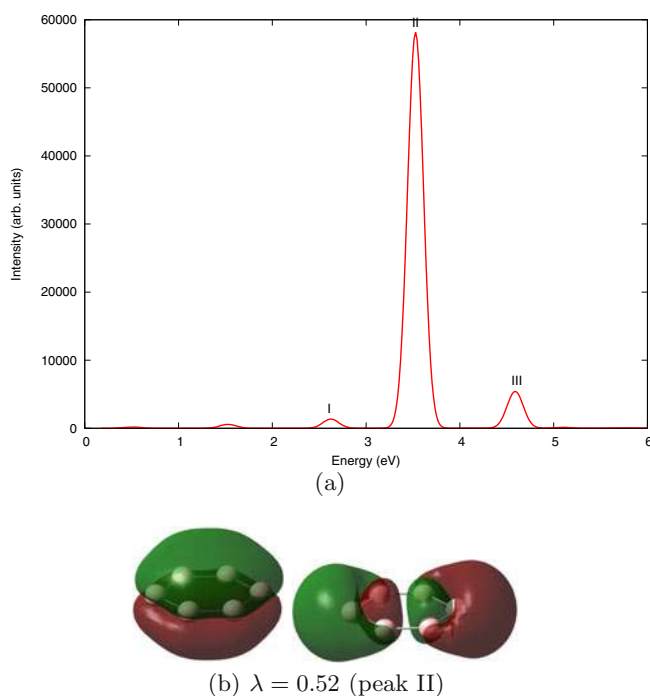


**Fig. 18.** The linear optical absorption spectrum of planar ring  $B_6^+$  isomer II, calculated using the CIS approach, along with the natural transition orbitals involved in the excited states corresponding to the peak II (3.52 eV). Parameter  $\lambda$  refers to a fraction of the NTO pair contribution to a given electronic excitation.

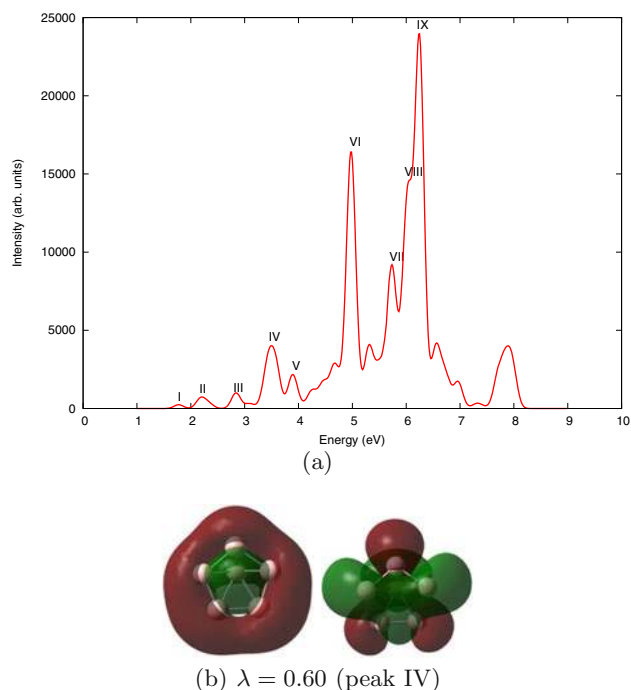


**Fig. 17.** The linear optical absorption spectrum of bulged wheel  $B_6^+$  isomer, calculated using the CIS approach, along with the natural transition orbitals involved in the excited states corresponding to the peak IV (3.58 eV). Parameter  $\lambda$  refers to a fraction of the NTO pair contribution to a given electronic excitation.

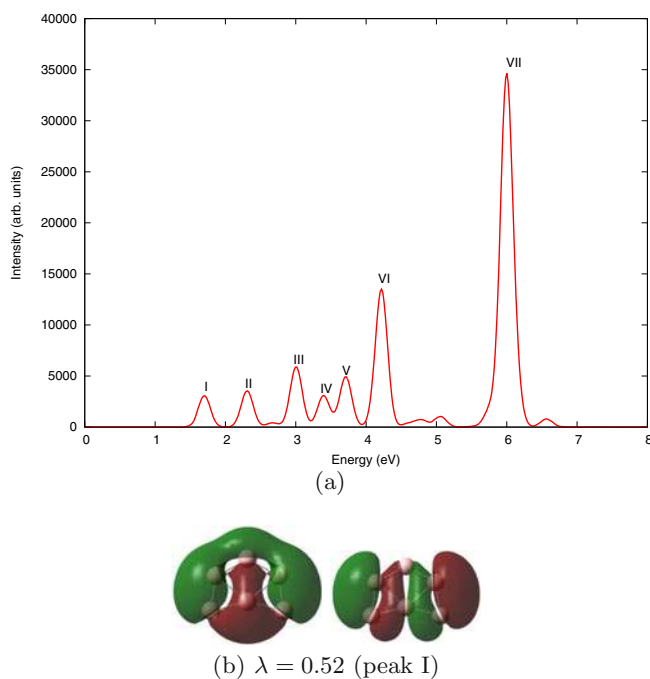
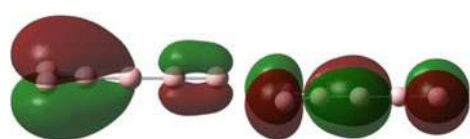
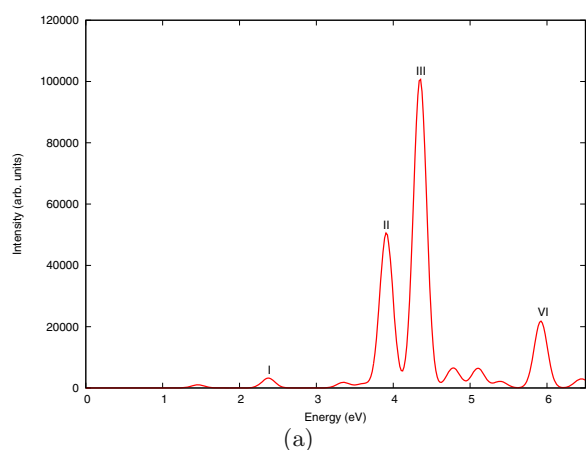
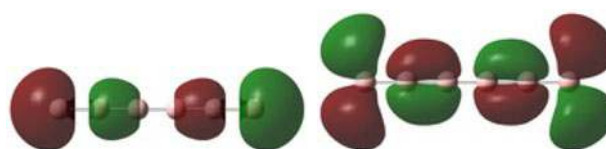
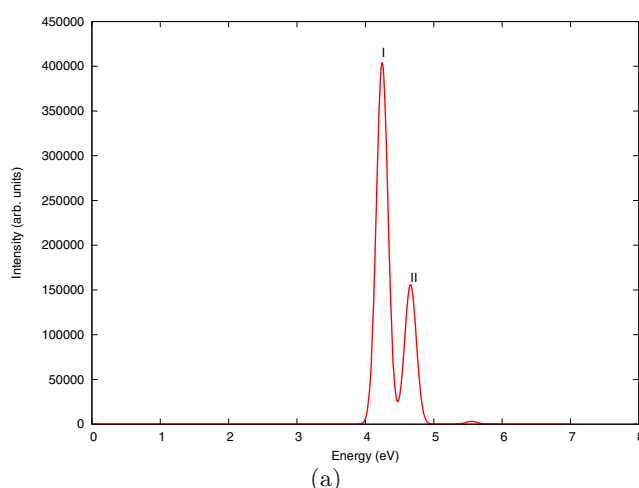


**Fig. 19.** The linear optical absorption spectrum of incomplete wheel  $B_6^+$  isomer, calculated using the CIS approach, along with the natural transition orbitals involved in the excited states corresponding to the peak I (1.69 eV). Parameter  $\lambda$  refers to a fraction of the NTO pair contribution to a given electronic excitation.



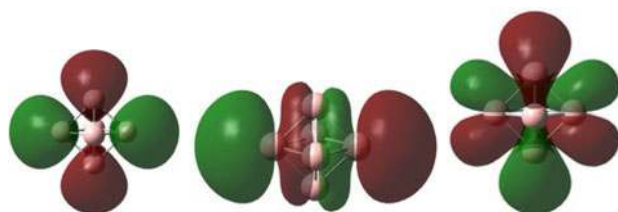
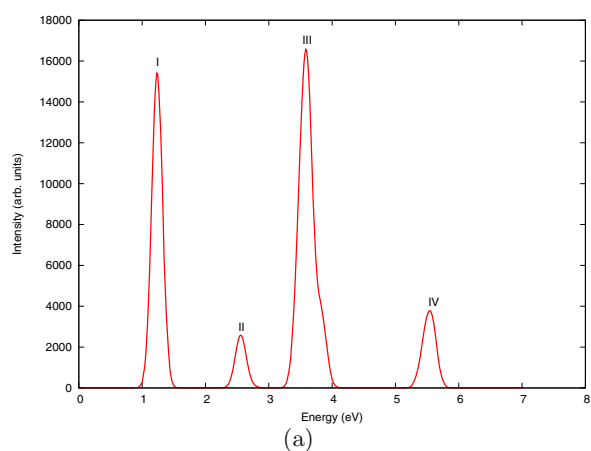
(b)  $\lambda = 0.93$  (peak II)

**Fig. 20.** The linear optical absorption spectrum of threaded trimer  $B_6^+$  isomer, calculated using the CIS approach, along with the natural transition orbitals involved in the excited states corresponding to the peak II (3.90 eV). Parameter  $\lambda$  refers to a fraction of the NTO pair contribution to a given electronic excitation.



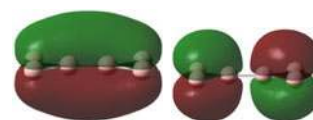
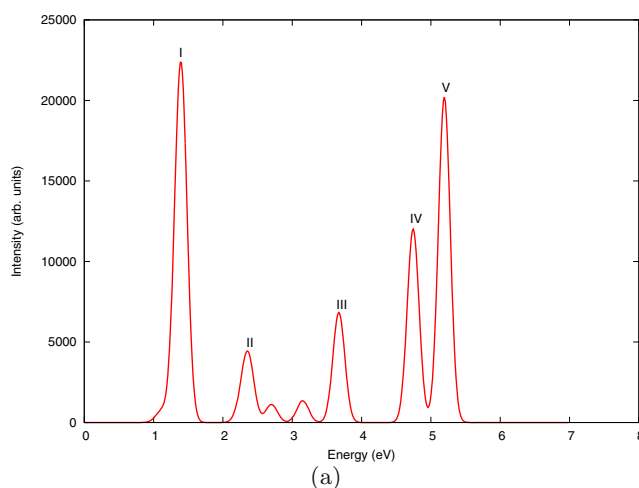
(b)  $\lambda = 0.44$  (peak I)

**Fig. 22.** The linear optical absorption spectrum of linear  $B_6^+$  isomer, calculated using the CIS approach, along with the natural transition orbitals involved in the excited states corresponding to the peak I (4.25 eV). Parameter  $\lambda$  refers to a fraction of the NTO pair contribution to a given electronic excitation.



(b)  $\lambda = 0.86$  (peak I),  $hole_1 \rightarrow particle_1, particle_2$

**Fig. 21.** The linear optical absorption spectrum of triangular bipyramid  $B_6^+$  isomer, calculated using the CIS approach, along with the natural transition orbitals involved in the excited states corresponding to the peak I (1.23 eV). Parameter  $\lambda$  refers to a fraction of the NTO pair contribution to a given electronic excitation.



(b)  $\lambda = 0.62$  (peak I)

**Fig. 23.** The linear optical absorption spectrum of planar trimers  $B_6^+$  isomer, calculated using the CIS approach, along with the natural transition orbitals involved in the excited states corresponding to the peak I (1.40 eV). Parameter  $\lambda$  refers to a fraction of the NTO pair contribution to a given electronic excitation.

of both neutral and cationic isomers are reported here. A singles configuration interaction approach was used to compute excited state energies and the absorption spectra of various clusters. Spectra of cationic clusters appear slightly red-shifted with respect to the neutral one. A comparison of spectra with CIS as well as more sophisticated EOM-CCSD method is presented in light of nature of excitations involved in the spectra. In all closed shell systems, a complete agreement on the nature of configurations involved is observed in both methods. On the other hand, for open-shell systems, minor contribution from double excitations are observed. Also, the spectra computed using EOM-CCSD approach is generally red-shifted as compared to the CIS ones. Such comparisons can be used to benchmark the CIS results.

Different isomers exhibit distinct optical response, even though they are isoelectronic and many of them are almost degenerate. This signals a strong-structure property relationship, which can be exploited for experimental identification of these isomers; something which is not possible with the conventional mass spectrometry. A strong mixture of configurations in the many-body wavefunctions of various excited states are observed, indicating the plasmonic nature of the photoexcited states [35].

Since aluminum also has the same number of valence electrons, it will be interesting to compute its optical absorption spectra, and compare them with those of boron cluster with the help of many-body wavefunctional analysis. The results of such calculations done by us will be communicated in near future [37].

The author (R.S.) would like to acknowledge the Council of Scientific and Industrial Research (CSIR), India, for their financial support (SRF award No. 09/087/(0600)2010-EMR-I and travel Grant No. TG/6939/12-HRD). We thank National Param Supercomputing Facility of CDAC, India for providing resources.

## Appendix: Excited state CI wavefunctions, energies and oscillator strengths

In the following tables, we have given the excitation energies (with respect to the ground state), and the many body wavefunctions of the excited states, corresponding to the peaks in the CIS photoabsorption spectra of various isomers listed in Figures 1 and 15, along with the oscillator strength  $f_{12}$  of the transitions,

$$f_{12} = \frac{2}{3} \frac{m_e}{\hbar^2} (E_2 - E_1) \sum_i |\langle m|d_i|G\rangle|^2 \quad (\text{A.1})$$

where,  $|m\rangle$  denotes the excited state in question,  $|G\rangle$ , the ground state, and  $d_i$  is the  $i$ th Cartesian component of the electric dipole operator. The single excitations are with respect to the reference state as given in respective tables.

Similar tables corresponding to the results of select EOM-CCSD calculations are also given below.

**Table A.1.** Excitation energies,  $E$ , and many-particle wavefunctions of excited states corresponding to the peaks in the CIS linear absorption spectrum of B<sub>6</sub>-planar ring (triplet) isomer (cf. Fig. 2). The subscript  $\parallel$  in the peak number denotes the absorption due to light polarized in the plane of isomer. In the wavefunction, the bracketed numbers are the CI coefficients of a given electronic configuration. Symbols  $H_{1\alpha}$  and  $H_{2\alpha}$  denote SOMOs discussed earlier, and  $H$ , and  $L$ , denote HOMO and LUMO orbitals, respectively. Note that, the reference state does not correspond to any peak, instead it represents the reference state from which singles excitations are occurring.

Peak	$E$ (eV)	$f_{12}$	$\langle S^2 \rangle$	Wavefunction
Reference				$ H_{1\alpha}^1; H_{2\alpha}^1\rangle$
I $\parallel$	2.85	0.0099	3.01	$ H_{\alpha} - 2 \rightarrow L_{\alpha}\rangle(0.6589)$ $ H_{1\alpha} \rightarrow L_{\alpha}\rangle(0.6102)$
II $\parallel$	3.42	0.0634	2.90	$ H_{1\alpha} \rightarrow L_{\alpha}\rangle(0.5415)$ $ H_{\beta} \rightarrow L_{\beta}\rangle(0.4719)$
III $\parallel$	4.31	0.0306	2.78	$ H_{\beta} - 1 \rightarrow L_{\beta} + 1\rangle(0.7253)$ $ H_{\beta} - 2 \rightarrow L_{\beta} + 12\rangle(0.3011)$
IV $\parallel$	4.62	0.1830	3.30	$ H_{\beta} - 3 \rightarrow L_{\beta} + 1\rangle(0.6176)$ $ H_{2\alpha} \rightarrow L_{\alpha} + 10\rangle(0.3007)$
V $\parallel$	4.98	0.1673	2.94	$ H_{\beta} - 3 \rightarrow L_{\beta} + 1\rangle(0.4591)$ $ H_{\beta} - 2 \rightarrow L_{\beta} + 16\rangle(0.3334)$
VI $\parallel$	5.89	0.3505	2.99	$ H_{\alpha} - 3 \rightarrow L_{\alpha} + 1\rangle(0.4911)$ $ H_{2\alpha} \rightarrow L_{\alpha} + 5\rangle(0.3587)$
VII $\parallel$	6.45	0.2201	3.31	$ H_{\alpha} - 5 \rightarrow L_{\alpha}\rangle(0.3976)$ $ H_{\alpha} - 3 \rightarrow L_{\alpha} + 1\rangle(0.3848)$
VIII $\parallel$	6.81	0.1848	2.88	$ H_{2\alpha} \rightarrow L_{\alpha} + 10\rangle(0.4423)$ $ H_{\beta} - 1 \rightarrow L_{\beta} + 3\rangle(0.3970)$

**Table A.2.** Excitation energies,  $E$ , and many-particle wavefunctions of excited states corresponding to the peaks in the EOM-CCSD linear absorption spectrum of B<sub>6</sub>-planar ring (triplet) isomer (cf. Fig. 3). The subscript  $\parallel$  in the peak number denotes the absorption due to light polarized in the plane of isomer. In the wavefunction, the bracketed numbers are the coupled-cluster amplitudes of a given electronic configuration. Symbols  $H_{1\alpha}$  and  $H_{2\alpha}$  denote SOMOs discussed earlier, and  $H$ , and  $L$ , denote HOMO and LUMO orbitals, respectively. Note that, the reference state does not correspond to any peak, instead it represents the reference state from which singles excitations are occurring.

Peak	$E$ (eV)	$f_{12}$	Wavefunction
Reference			$ H_{1\alpha}^1; H_{2\alpha}^1\rangle$
I $\parallel$	1.74	0.0179	$ H_{1\alpha} \rightarrow L_{\alpha}\rangle(0.7968)$ $ H_{\alpha} - 2 \rightarrow L_{\alpha}\rangle(0.2623)$ $ H_{\alpha} - 1 \rightarrow L_{\alpha}; H_{\beta} - 1 \rightarrow L_{\beta} + 1\rangle$ $(0.1149)$

**Table A.2.** Continued.

Peak	$E$ (eV)	$f_{12}$	Wavefunction
II <sub>  </sub>	2.71	0.0082	$ H_\beta \rightarrow L_\beta\rangle(0.6442)$ $ H_{1\alpha} \rightarrow L_\alpha\rangle(0.2320)$
III <sub>  </sub>	3.20	0.0603	$ H_\beta - 1 \rightarrow L_\beta + 1\rangle(0.3111)$ $ H_\beta - 2 \rightarrow L_\beta\rangle(0.4768)$
IV <sub>  </sub>	3.50	0.0371	$ H_\beta - 3 \rightarrow L_\beta + 1\rangle(0.5933)$ $ H_{2\alpha} \rightarrow L_\alpha + 10\rangle(0.1421)$
V <sub>  </sub>	4.03	0.0046	$ H_\beta - 3 \rightarrow L_\beta + 1\rangle(0.2861)$ $ H_\beta - 2 \rightarrow L_\beta + 16\rangle(0.1968)$ $ H_{1\alpha} \rightarrow L_\alpha; H_\beta - 2 \rightarrow L_\beta + 1\rangle$ (0.1102)
VI <sub>  </sub>	5.05	0.4106	$ H_{2\alpha} \rightarrow L_\alpha + 5\rangle(0.3573)$ $ H_\alpha - 3 \rightarrow L_\alpha + 1\rangle(0.1820)$ $ H_{1\alpha} \rightarrow L_\alpha; H_\beta - 2 \rightarrow L_\beta + 1\rangle$ (0.1612)
VII <sub>  </sub>	5.50	0.0801	$ H_\alpha - 5 \rightarrow L_\alpha\rangle(0.2023)$ $ H_\alpha - 4 \rightarrow L_\alpha + 7\rangle(0.1358)$ $ H_\alpha - 1 \rightarrow L_\alpha; H_\beta - 3 \rightarrow L_\beta + 1\rangle$ (0.1157) $ H_{1\alpha} \rightarrow L_\alpha; H_\beta - 3 \rightarrow L_\beta + 16\rangle$ (0.1025)

**Table A.3.** Excitation energies,  $E$ , and many-particle wavefunctions of excited states corresponding to the peaks in the CIS linear absorption spectrum of B<sub>6</sub>-incomplete wheel isomer (cf. Fig. 4). The subscripts || and  $\perp$ , in the peak number denote the absorption due to light polarized in, and perpendicular to the plane of wheel base, respectively. The rest of the information is the same as given in the caption for Table A.1.

Peak	$E$ (eV)	$f_{12}$	$\langle S^2 \rangle$	Wavefunction
Reference				$ H_{1\alpha}^1; H_{2\alpha}^1\rangle$
I <sub>  </sub>	3.09	0.0447	2.68	$ H_{1\alpha} \rightarrow L_\alpha\rangle(0.6251)$ $ H_{2\alpha} \rightarrow L_\alpha + 1\rangle(0.5904)$
II <sub>  </sub>	3.55	0.0346	2.83	$ H_\alpha - 2 \rightarrow L_\alpha\rangle(0.8721)$
III <sub><math>\perp</math></sub>	3.85	0.0623	2.69	$ H_\beta \rightarrow L_\beta\rangle(0.9095)$ $ H_\beta \rightarrow L_\beta + 11\rangle(0.2045)$
IV <sub>  </sub>	4.96	0.0651	3.00	$ H_\beta \rightarrow L_\beta + 2\rangle(0.3971)$ $ H_\alpha - 3 \rightarrow L_\alpha + 1\rangle(0.3695)$
V <sub>  </sub>	5.77	0.0320	2.817	$ H_{2\alpha} \rightarrow L_\alpha + 25\rangle(0.5802)$ $ H_{2\alpha} \rightarrow L_\alpha + 7\rangle(0.3785)$
VI <sub>  </sub>	6.35	0.2942	3.10	$ H_{2\alpha} \rightarrow L_\alpha + 7\rangle(0.5776)$ $ H_\alpha - 5 \rightarrow L_\alpha\rangle(0.3245)$
VII <sub>  </sub>	6.69	0.0321	2.82	$ H_{2\alpha} \rightarrow L_\alpha + 2\rangle(0.7301)$ $ H_{2\alpha} \rightarrow L_\alpha + 5\rangle(0.4955)$

**Table A.4.** Excitation energies,  $E$ , and many-particle wavefunctions of excited states corresponding to the peaks in the CIS linear absorption spectrum of B<sub>6</sub>-bulged wheel isomer (cf. Fig. 5). The subscripts || and  $\perp$ , in the peak number denote the absorption due to light polarized in, and perpendicular to the plane of wheel base, respectively. In the wavefunction, the bracketed numbers are the CI coefficients of a given electronic configuration. Symbols  $H$  and  $L$  denote HOMO and LUMO orbitals, respectively. Excitations are with respect to the closed-shell Hartree-Fock reference state.

Peak	$E$ (eV)	$f_{12}$	Wavefunction
I <sub>  </sub>	3.76	0.2625	$ H - 1 \rightarrow L + 6\rangle(0.5622)$ $ H \rightarrow L + 6\rangle(0.5622)$ $ H - 1 \rightarrow L + 2\rangle(0.4459)$ $ H \rightarrow L + 2\rangle(0.4459)$
II <sub>  </sub>	4.38	0.0657	$ H - 1 \rightarrow L + 3\rangle(0.4998)$ $ H \rightarrow L + 3\rangle(0.4998)$ $ H - 1 \rightarrow L + 4\rangle(0.4981)$ $ H \rightarrow L + 4\rangle(0.4981)$
III <sub>  </sub>	5.07	2.1039	$ H - 2 \rightarrow L + 1\rangle(0.7653)$ $ H - 2 \rightarrow L\rangle(0.7653)$ $ H - 2 \rightarrow L + 8\rangle(0.2857)$ $ H - 2 \rightarrow L + 7\rangle(0.2857)$
IV <sub><math>\perp</math></sub>	5.71	0.0810	$ H - 2 \rightarrow L + 6\rangle(0.6266)$ $ H - 2 \rightarrow L + 2\rangle(0.5564)$
V <sub>  </sub>	7.05	1.0550	$ H \rightarrow L + 5\rangle(0.7645)$ $ H - 1 \rightarrow L + 5\rangle(0.7645)$ $ H \rightarrow L + 6\rangle(0.4763)$ $ H - 1 \rightarrow L + 6\rangle(0.4763)$

**Table A.5.** Excitation energies,  $E$ , and many-particle wavefunctions of excited states corresponding to the peaks in the EOM-CCSD linear absorption spectrum of B<sub>6</sub>-bulged wheel isomer (cf. Fig. 6) calculated using EOM-CCSD approach. The subscripts || and  $\perp$ , in the peak number denote the absorption due to light polarized in, and perpendicular to the plane of wheel base, respectively. In the wavefunction, the bracketed numbers are the coupled-cluster amplitudes of a given electronic configuration. Symbols  $H$  and  $L$  denote HOMO and LUMO orbitals, respectively. Excitations are with respect to the closed-shell Hartree-Fock reference state.

Peak	$E$ (eV)	$f_{12}$	Wavefunction
I <sub>  </sub>	3.21	0.0088	$ H - 1 \rightarrow L + 6\rangle(0.3898)$ $ H \rightarrow L + 6\rangle(0.3898)$ $ H - 1 \rightarrow L + 2\rangle(0.3519)$ $ H \rightarrow L + 2\rangle(0.3519)$

**Table A.5.** Continued.

Peak	$E$ (eV)	$f_{12}$	Wavefunction
II <sub>  </sub>	3.43	0.0256	$ H - 1 \rightarrow L + 3\rangle(0.3604)$ $ H \rightarrow L + 3\rangle(0.3604)$ $ H - 1 \rightarrow L + 4\rangle(0.3604)$ $ H \rightarrow L + 4\rangle(0.3604)$
III <sub>  </sub>	4.61	0.2658	$ H - 2 \rightarrow L + 1\rangle(0.5074)$ $ H - 2 \rightarrow L\rangle(0.5074)$ $ H - 2 \rightarrow L + 8\rangle(0.2183)$ $ H - 2 \rightarrow L + 7\rangle(0.2183)$
IV <sub>⊥</sub>	5.25	0.0004	$ H - 2 \rightarrow L + 6\rangle(0.3675)$ $ H - 2 \rightarrow L + 2\rangle(0.3473)$
V <sub>  </sub>	6.77	0.224	$ H \rightarrow L + 5\rangle(0.5106)$ $ H - 1 \rightarrow L + 5\rangle(0.5106)$ $ H \rightarrow L + 6\rangle(0.3575)$ $ H - 1 \rightarrow L + 6\rangle(0.3575)$

**Table A.6.** Excitation energies,  $E$ , and many-particle wavefunctions of excited states corresponding to the peaks in the CIS linear absorption spectrum of B<sub>6</sub>-planar ring (singlet) isomer (cf. Fig. 7). The subscripts || and ⊥, in the peak number denote the absorption due to light polarized in, and perpendicular to the plane of the isomer, respectively. The rest of the information is the same as given in the caption for Table A.4.

Peak	$E$ (eV)	$f_{12}$	Wavefunction
I <sub>  </sub>	3.12	0.5397	$ H - 1 \rightarrow L\rangle(0.9174)$ $ H \rightarrow L + 23\rangle(0.2504)$
II <sub>  </sub>	5.28	1.0153	$ H \rightarrow L + 7\rangle(0.4991)$ $ H \rightarrow L + 23\rangle(0.4093)$
III <sub>  </sub>	5.61	0.1380	$ H - 1 \rightarrow L + 2\rangle(0.5479)$ $ H - 1 \rightarrow L + 8\rangle(0.5181)$
IV <sub>  ,⊥</sub>	5.88	0.8199	$ H \rightarrow L + 7\rangle(0.7472)$ $ H \rightarrow L + 12\rangle(0.3140)$
V <sub>  </sub>	6.77	2.2212	$ H \rightarrow L + 16\rangle(0.4623)$ $ H \rightarrow L + 12\rangle(0.4600)$
VI <sub>  </sub>	7.15	0.6003	$ H \rightarrow L + 16\rangle(0.6363)$ $ H \rightarrow L + 12\rangle(0.5687)$

**Table A.7.** Excitation energies,  $E$ , and many-particle wavefunctions of excited states corresponding to the peaks in the CIS linear absorption spectrum of B<sub>6</sub>-octahedron isomer (cf. Fig. 8). The subscripts || and ⊥, in the peak number denote the absorption due to light polarized in, and perpendicular to the plane of pyramidal base, respectively. The rest of the information is the same as given in the caption for Table A.1.

Peak	$E$ (eV)	$f_{12}$	$\langle S^2 \rangle$	Wavefunction
Reference				$ H_{1\alpha}^1; H_{2\alpha}^1\rangle$
I <sub>  ,⊥</sub>	0.92	0.1110	2.25	$ H_{1\alpha} \rightarrow L_{\alpha}\rangle(0.8790)$ $ H_{2\alpha} \rightarrow L_{\alpha} + 2\rangle(0.8612)$ $ H_{2\alpha} \rightarrow L_{\alpha} + 1\rangle(0.6610)$ $ H_{1\alpha} \rightarrow L_{\alpha} + 1\rangle(0.6128)$
II <sub>  ,⊥</sub>	2.50	0.0111	3.37	$ H_{\alpha} - 2 \rightarrow L_{\alpha} + 1\rangle(0.6637)$ $ H_{\alpha} - 2 \rightarrow L_{\alpha} + 2\rangle(0.6637)$ $ H_{\alpha} - 1 \rightarrow L_{\alpha}\rangle(0.6637)$ $ H_{\alpha} - 1 \rightarrow L_{\alpha} + 1\rangle(0.6637)$
III <sub>  ,⊥</sub>	3.69	0.0111	3.65	$ H_{\alpha} - 4 \rightarrow L_{\alpha}\rangle(0.8186)$ $ H_{\alpha} - 4 \rightarrow L_{\alpha} + 1\rangle(0.8032)$ $ H_{\alpha} - 4 \rightarrow L_{\alpha} + 2\rangle(0.8032)$ $ H_{\beta} \rightarrow L_{\beta} + 2\rangle(0.3117)$
IV <sub>  ,⊥</sub>	4.69	0.5265	2.55	$ H_{\beta} \rightarrow L_{\beta} + 2\rangle(0.5448)$ $ H_{\beta} \rightarrow L_{\beta} + 3\rangle(0.5448)$ $ H_{\beta} \rightarrow L_{\beta} + 4\rangle(0.5448)$ $ H_{\beta} \rightarrow L_{\beta} + 10\rangle(0.3673)$

**Table A.8.** Excitation energies,  $E$ , and many-particle wavefunctions of excited states corresponding to the peaks in the CIS linear absorption spectrum of B<sub>6</sub>-threaded tetramer isomer (cf. Fig. 9). The subscript  $x$  in the peak number denote the absorption due to light polarized along the long axis, and,  $y, z$  denotes polarization perpendicular to it. The rest of the information is the same as given in the caption for Table A.1.

Peak	$E$ (eV)	$f_{12}$	$\langle S^2 \rangle$	Wavefunction
Reference				$ H_{1\alpha}^1; H_{2\alpha}^1\rangle$
I <sub><math>x</math></sub>	3.06	0.0297	2.61	$ H_{2\alpha} \rightarrow L_{\alpha} + 2\rangle(0.7532)$ $ H_{\beta} \rightarrow L_{\beta} + 1\rangle(0.2966)$
II <sub><math>x</math></sub>	4.03	0.0687	2.07	$ H_{1\alpha} \rightarrow L_{\alpha} + 2\rangle(0.5156)$ $ H_{\beta} \rightarrow L_{\beta}\rangle(0.3829)$ $ H_{\beta} - 1 \rightarrow L_{\beta} + 2\rangle(0.3347)$
III <sub><math>z</math></sub>	4.48	0.3363	2.05	$ H_{\beta} \rightarrow L_{\beta} + 2\rangle(0.6089)$ $ H_{2\alpha} \rightarrow L_{\alpha} + 1\rangle(0.5316)$
IV <sub><math>z</math></sub>	5.67	0.0283	3.13	$ H_{\beta} \rightarrow L_{\beta} + 5\rangle(0.5808)$ $ H_{\beta} \rightarrow L_{\beta} + 20\rangle(0.4305)$
V <sub><math>y</math></sub>	6.16	0.0384	2.05	$ H_{1\alpha} \rightarrow L_{\alpha} + 3\rangle(0.5497)$ $ H_{1\alpha} \rightarrow L_{\alpha} + 5\rangle(0.5357)$
VI <sub><math>y</math></sub>	6.36	0.2072	2.32	$ H_{\beta} - 3 \rightarrow L_{\beta}\rangle(0.5076)$ $ H_{\beta} - 1 \rightarrow L_{\beta} + 2\rangle(0.2922)$

**Table A.9.** Excitation energies,  $E$ , and many-particle wavefunctions of excited states corresponding to the peaks in the CIS linear absorption spectrum of B<sub>6</sub>-threaded trimer isomer (cf. Fig. 10). The subscript  $\parallel$ , in the peak number denotes the absorption due to light polarized along the long axis of the isomer. The rest of the information is the same as given in the caption for Table A.1.

Peak	$E$ (eV)	$f_{12}$	$\langle S^2 \rangle$	Wavefunction
Reference				$ H_{1\alpha}^1; H_{2\alpha}^1\rangle$
I $\parallel$	1.16	0.0063	2.08	$ H_{\beta} - 1 \rightarrow L_{\beta}\rangle(0.6839)$ $ H_{\alpha} - 1 \rightarrow L_{\alpha}\rangle(0.6061)$
II $\parallel$	2.28	0.0313	2.083	$ H_{\alpha} - 2 \rightarrow L_{\alpha}\rangle(0.6226)$ $ H_{\beta} - 2 \rightarrow L_{\beta}\rangle(0.6329)$
III $\parallel$	3.06	0.0214	2.12	$ H_{2\alpha} \rightarrow L_{\alpha}\rangle(0.6536)$ $ H_{\beta} \rightarrow L_{\beta}\rangle(0.5487)$
IV $\parallel$	4.03	0.6573	2.08	$ H_{\beta} \rightarrow L_{\beta} + 1\rangle(0.5280)$ $ H_{2\alpha} \rightarrow L_{\alpha} + 1\rangle(0.4969)$
V $\parallel$	4.73	0.596	2.99	$ H_{\beta} \rightarrow L_{\beta} + 7\rangle(0.3826)$ $ H_{\alpha} - 3 \rightarrow L_{\alpha} + 1\rangle(0.3516)$
VI $\parallel$	5.37	0.1391	2.07	$ H_{2\alpha} \rightarrow L_{\alpha} + 7\rangle(0.5799)$ $ H_{\beta} \rightarrow L_{\beta} + 8\rangle(0.4231)$
VII $\parallel$	5.69	0.2293	2.19	$ H_{\beta} \rightarrow L_{\beta} + 4\rangle(0.5125)$ $ H_{2\alpha} \rightarrow L_{\alpha} + 3\rangle(0.4084)$

**Table A.10.** Excitation energies,  $E$ , and many-particle wavefunctions of excited states corresponding to the peaks in the CIS linear absorption spectrum of B<sub>6</sub>-twisted trimers isomer (cf. Fig. 11). The subscripts  $\parallel$  and  $\perp$ , in the peak number denote the absorption due to light polarized along, and perpendicular to the long axis of the isomer, respectively. The rest of the information is the same as given in the caption for Table A.4.

Peak	$E$ (eV)	$f_{12}$	Wavefunction
I $\parallel$	1.02	0.0422	$ H \rightarrow L\rangle(0.6550)$ $ H - 1 \rightarrow L\rangle(0.6550)$ $ H \rightarrow L + 1\rangle(0.5612)$ $ H - 1 \rightarrow L + 1\rangle(0.5612)$
II $\perp$	2.22	0.1279	$ H - 2 \rightarrow L\rangle(0.7650)$ $ H - 3 \rightarrow L + 1\rangle(0.5316)$
III $\parallel$	3.58	0.1870	$ H - 2 \rightarrow L + 2\rangle(0.4374)$ $ H - 5 \rightarrow L\rangle(0.4374)$ $ H - 4 \rightarrow L\rangle(0.4371)$ $ H - 2 \rightarrow L + 3\rangle(0.4371)$
IV $\parallel$	4.72	0.4337	$ H - 2 \rightarrow L + 2\rangle(0.4874)$ $ H - 2 \rightarrow L + 3\rangle(0.4874)$ $ H \rightarrow L + 26\rangle(0.3268)$ $ H - 1 \rightarrow L + 26\rangle(0.3268)$

**Table A.10.** Continued.

Peak	$E$ (eV)	$f_{12}$	Wavefunction
V $\perp$	5.26	0.3570	$ H - 5 \rightarrow L + 3\rangle(0.5117)$ $ H - 4 \rightarrow L + 2\rangle(0.5010)$
VI $\perp$	5.87	3.4368	$ H \rightarrow L + 3\rangle(0.5962)$ $ H - 1 \rightarrow L + 2\rangle(0.5962)$
VII $\parallel$	6.39	0.2265	$ H - 3 \rightarrow L + 2\rangle(0.4908)$ $ H - 3 \rightarrow L + 3\rangle(0.4908)$ $ H - 2 \rightarrow L + 3\rangle(0.4561)$ $ H - 2 \rightarrow L + 2\rangle(0.4561)$
VIII $\perp$	6.98	0.6645	$ H - 3 \rightarrow L + 1\rangle(0.6479)$ $ H - 2 \rightarrow L\rangle(0.5508)$
IX $\parallel$	7.25	0.3140	$ H \rightarrow L + 4\rangle(0.5209)$ $ H - 1 \rightarrow L + 4\rangle(0.5209)$ $ H \rightarrow L + 7\rangle(0.4072)$ $ H - 1 \rightarrow L + 7\rangle(0.4072)$

**Table A.11.** Excitation energies,  $E$ , and many-particle wavefunctions of excited states corresponding to the peaks in the CIS linear absorption spectrum of B<sub>6</sub>-planar trimers isomer (cf. Fig. 12). The subscripts  $\parallel$  and  $\perp$ , in the peak number denote the absorption due to light polarized in, and perpendicular to the plane of the isomer, respectively. The rest of the information is the same as given in the caption for Table A.4.

Peak	$E$ (eV)	$f_{12}$	Wavefunction
I $\perp$	0.97	0.0393	$ H \rightarrow L\rangle(0.7804)$ $ H - 1 \rightarrow L + 1\rangle(0.5529)$
II $\parallel$	2.22	0.1261	$ H - 2 \rightarrow L\rangle(0.7603)$ $ H - 4 \rightarrow L + 1\rangle(0.5634)$
III $\parallel$	3.57	0.1293	$ H - 2 \rightarrow L + 2\rangle(0.6070)$ $ H - 3 \rightarrow L\rangle(0.5440)$
IV $\parallel$	4.67	0.7257	$ H - 3 \rightarrow L + 2\rangle(0.7242)$ $ H \rightarrow L + 12\rangle(0.3824)$ $ H - 2 \rightarrow L + 2\rangle(0.5131)$ $ H - 3 \rightarrow L\rangle(0.4653)$
V $\parallel$	6.43	4.5721	$ H \rightarrow L + 12\rangle(0.5256)$ $ H - 3 \rightarrow L + 2\rangle(0.4859)$
VI $\parallel$	6.99	1.8466	$ H - 4 \rightarrow L + 1\rangle(0.5794)$ $ H \rightarrow L + 7\rangle(0.5156)$
VII $\parallel$	7.34	0.6386	$ H \rightarrow L + 12\rangle(0.6754)$ $ H \rightarrow L + 7\rangle(0.4922)$

**Table A.12.** Excitation energies,  $E$ , and many-particle wavefunctions of excited states corresponding to the peaks in the CIS linear absorption spectrum of B<sub>6</sub>-convex bowl isomer (cf. Fig. 13). The subscripts  $\parallel$  and  $\perp$ , in the peak number denote the absorption due to light polarized in, and perpendicular to the plane of the isomer, respectively. The rest of the information is the same as given in the caption for Table A.4.

Peak	$E$ (eV)	$f_{12}$	Wavefunction
I $\parallel$	1.58	0.0486	$ H - 1 \rightarrow L + 1\rangle$ (0.9774)
II $\parallel,\perp$	1.80	0.0679	$ H \rightarrow L + 2\rangle$ (0.9079) $ H - 1 \rightarrow L + 3\rangle$ (0.2748)
III $\parallel$	2.43	0.6023	$ H \rightarrow L\rangle$ (0.8644) $ H - 4 \rightarrow L + 1\rangle$ (0.4364)
IV $\parallel$	2.89	0.1811	$ H - 1 \rightarrow L\rangle$ (0.8058) $ H - 3 \rightarrow L + 1\rangle$ (0.5421)
V $\parallel$	4.09	0.1602	$ H - 4 \rightarrow L\rangle$ (0.5608) $ H - 3 \rightarrow L + 1\rangle$ (0.5347)
VI $\parallel,\perp$	5.13	0.0649	$ H - 4 \rightarrow L + 3\rangle$ (0.9070) $ H - 3 \rightarrow L + 2\rangle$ (0.1753)
VII $\parallel$	6.21	1.4363	$ H \rightarrow L + 7\rangle$ (0.4118) $ H \rightarrow L + 4\rangle$ (0.3622)
VIII $\perp$	6.39	2.2019	$ H \rightarrow L + 6\rangle$ (0.4335) $ H - 2 \rightarrow L + 3\rangle$ (0.4081)
IX $\parallel$	6.90	0.1476	$ H \rightarrow L + 8\rangle$ (0.4435) $ H \rightarrow L + 13\rangle$ (0.3534)

**Table A.13.** Excitation energies,  $E$ , and many-particle wavefunctions of excited states corresponding to the peaks in the CIS linear absorption spectrum of B<sub>6</sub>-linear isomer (cf. Fig. 14). The subscripts  $\parallel$  and  $\perp$ , in the peak number denote the absorption due to light polarized along, and perpendicular to the axis of the isomer, respectively. The rest of the information is the same as given in the caption for Table A.4.

Peak	$E$ (eV)	$f_{12}$	Wavefunction
I $\parallel$	5.51	12.8358	$ H - 1 \rightarrow L + 3\rangle$ (0.6510) $ H \rightarrow L + 2\rangle$ (0.6489)
II $\perp$	6.51	1.6532	$ H \rightarrow L + 4\rangle$ (0.7148) $ H - 1 \rightarrow L + 4\rangle$ (0.7148) $ H - 3 \rightarrow L + 8\rangle$ (0.3847) $ H - 2 \rightarrow L + 8\rangle$ (0.3847)

**Table A.14.** Excitation energies,  $E$ , and many-particle wavefunctions of excited states corresponding to the peaks in the CIS linear absorption spectrum of B<sub>6</sub><sup>+</sup>-planar ring isomer (cf. Fig. 16). The subscripts  $\parallel$  and  $\perp$ , in the peak number denote the absorption due to light polarized in, and perpendicular to the plane of the isomer, respectively. In the wavefunction, the bracketed numbers are the CI coefficients of a given electronic configuration. Symbols  $H$ ,  $H_1$  and  $L$  denote HOMO, SOMO and LUMO orbitals, respectively.

Peak	$E$ (eV)	$f_{12}$	$\langle S^2 \rangle$	Wavefunction
Reference				$ H_{1\alpha}^1\rangle$
I $\perp$	4.44	0.4236	0.84	$ H_\beta - 1 \rightarrow L_\beta\rangle$ (0.5530) $ H_\alpha - 1 \rightarrow L_\alpha\rangle$ (0.5077)
II $\parallel$	5.32	0.1504	1.02	$ H_\beta - 1 \rightarrow L_\beta + 3\rangle$ (0.4780) $ H_\alpha - 3 \rightarrow L_\alpha + 3\rangle$ (0.4433)
III $\parallel$	6.09	0.0987	0.88	$ H_\alpha - 5 \rightarrow L_\alpha\rangle$ (0.5713) $ H_\beta - 4 \rightarrow L_\beta\rangle$ (0.5595)
IV $\parallel$	6.85	0.8066	0.87	$ H_{1\alpha} \rightarrow L_\alpha + 6\rangle$ (0.6347) $ H_\alpha \rightarrow L_\alpha + 9\rangle$ (0.3584)

**Table A.15.** Excitation energies,  $E$ , and many-particle wavefunctions of excited states corresponding to the peaks in the CIS linear absorption spectrum of B<sub>6</sub><sup>+</sup>-bulged wheel isomer (cf. Fig. 17). The subscripts  $\parallel$  and  $\perp$ , in the peak number denote the absorption due to light polarized in, and perpendicular to the plane of the wheel, respectively. The rest of the information is the same as given in the caption for Table A.14.

Peak	$E$ (eV)	$f_{12}$	$\langle S^2 \rangle$	Wavefunction
Reference				$ H_{1\alpha}^1\rangle$
I $\parallel$	1.76	0.0018	1.53	$ H_\beta \rightarrow L_\beta\rangle$ (0.7618) $ H_\beta - 1 \rightarrow L_\beta\rangle$ (0.5218)
II $\parallel$	2.19	0.0049	1.02	$ H_\beta - 1 \rightarrow L_\beta\rangle$ (0.8082) $ H_\beta \rightarrow L_\beta\rangle$ (0.5406)
III $\parallel$	2.84	0.0074	2.43	$ H_{1\alpha} \rightarrow L_\alpha\rangle$ (0.5381) $ H_\beta \rightarrow L_\beta + 1\rangle$ (0.4385)
IV $\parallel$	3.58	0.0183	1.80	$ H_\alpha - 2 \rightarrow L_\alpha + 7\rangle$ (0.4521) $ H_{1\alpha} \rightarrow L_\alpha\rangle$ (0.4594)
V $\parallel$	3.90	0.0114	1.74	$ H_{1\alpha} \rightarrow L_\alpha + 1\rangle$ (0.6233) $ H_\alpha - 2 \rightarrow L_\alpha + 2\rangle$ (0.5090)
VI $\parallel$	4.97	0.1173	1.98	$ H_\alpha - 1 \rightarrow L_\alpha\rangle$ (0.5925) $ H_\alpha - 3 \rightarrow L_\alpha\rangle$ (0.3915)

**Table A.15.** Continued.

Peak	$E$ (eV)	$f_{12}$	$\langle S^2 \rangle$	Wavefunction
VII <sub>  </sub>	5.74	0.0364	2.04	$ H_\alpha - 4 \rightarrow L_\alpha + 1\rangle(0.3974)$ $ H_\alpha - 2 \rightarrow L_\alpha + 3\rangle(0.3930)$
VIII <sub>  </sub>	6.05	0.0054	2.19	$ H_\alpha - 4 \rightarrow L_\alpha + 1\rangle(0.4416)$ $ H_\alpha - 3 \rightarrow L_\alpha\rangle(0.3428)$
IX <sub>  ,⊥</sub>	6.24	0.1731	1.53	$ H_\beta - 2 \rightarrow L_\beta + 2\rangle(0.4368)$ $ H_\alpha - 1 \rightarrow L_\alpha + 3\rangle(0.3700)$

**Table A.16.** Excitation energies,  $E$ , and many-particle wavefunctions of excited states corresponding to the peaks in the CIS linear absorption spectrum of B<sub>6</sub><sup>+</sup>-planar ring (II) isomer (cf. Fig. 18). The subscript || in the peak number denote the absorption due to light polarized in the plane of the isomer. The rest of the information is the same as given in the caption for Table A.14.

Peak	$E$ (eV)	$f_{12}$	$\langle S^2 \rangle$	Wavefunction
Reference				$ H_{1\alpha}^1\rangle$
I <sub>  </sub>	2.62	0.0100	2.30	$ H_\beta - 2 \rightarrow L_\beta + 2\rangle(0.8930)$ $ H_\alpha - 2 \rightarrow L_\alpha + 1\rangle(0.3196)$
II <sub>  </sub>	3.52	0.4311	0.86	$ H_\beta - 1 \rightarrow L_\beta\rangle(0.5075)$ $ H_\beta - 2 \rightarrow L_\beta + 1\rangle(0.5047)$
III <sub>  </sub>	4.59	0.0377	0.96	$ H_\beta - 3 \rightarrow L_\beta\rangle(0.6407)$ $ H_\alpha - 4 \rightarrow L_\alpha\rangle(0.4707)$

**Table A.17.** Excitation energies,  $E$ , and many-particle wavefunctions of excited states corresponding to the peaks in the CIS linear absorption spectrum of B<sub>6</sub><sup>+</sup>-incomplete wheel (quartet) isomer (cf. Fig. 19). The subscripts || and ⊥, in the peak number denote the absorption due to light polarized in, and perpendicular to the plane of the isomer, respectively. In the wavefunction, the bracketed numbers are the CI coefficients of a given electronic configuration. Symbols  $H$ ,  $H_{1\alpha}$ ,  $H_{2\alpha}$ ,  $H_{3\alpha}$  and  $L$  denote HOMO, SOMOs and LUMO orbitals, respectively.

Peak	$E$ (eV)	$f_{12}$	$\langle S^2 \rangle$	Wavefunction
Reference				$ H_{1\alpha}^1; H_{2\alpha}^1; H_{3\alpha}^1\rangle$
I <sub>⊥</sub>	1.69	0.0228	4.38	$ H_\beta - 2 \rightarrow L_\beta\rangle(0.7070)$ $ H_\beta - 1 \rightarrow L_\beta\rangle(0.5707)$
II <sub>  </sub>	2.31	0.0263	4.27	$ H_\beta - 2 \rightarrow L_\beta\rangle(0.6484)$ $ H_\beta - 1 \rightarrow L_\beta\rangle(0.5313)$
III <sub>⊥</sub>	3.00	0.0438	4.35	$ H_\alpha - 1 \rightarrow L_\alpha\rangle(0.6704)$ $ H_{2\alpha} \rightarrow L_\alpha\rangle(0.3992)$
IV <sub>  </sub>	3.39	0.0227	4.64	$ H_{1\alpha} \rightarrow L_\alpha\rangle(0.8546)$ $ H_{2\alpha} \rightarrow L_\alpha + 2\rangle(0.2748)$
V <sub>  </sub>	3.71	0.0365	4.32	$ H_{3\alpha} \rightarrow L_\alpha + 1\rangle(0.5299)$ $ H_\alpha - 1 \rightarrow L_\alpha\rangle(0.5106)$

**Table A.17.** Continued.

Peak	$E$ (eV)	$f_{12}$	$\langle S^2 \rangle$	Wavefunction
VI <sub>  </sub>	4.21	0.0987	4.56	$ H_\beta \rightarrow L_\beta + 1\rangle(0.8754)$ $ H_{3\alpha} \rightarrow L_\alpha + 9\rangle(0.2200)$
VII <sub>⊥</sub>	5.99	0.2462	5.33	$ H_\beta - 1 \rightarrow L_\beta + 5\rangle(0.5679)$ $ H_{3\alpha} \rightarrow L_\alpha + 4\rangle(0.4243)$

**Table A.18.** Excitation energies,  $E$ , and many-particle wavefunctions of excited states corresponding to the peaks in the CIS linear absorption spectrum of B<sub>6</sub><sup>+</sup>-threaded trimer (quartet) isomer (cf. Fig. 20). The subscripts || and ⊥, in the peak number denote the absorption due to light polarized along, and perpendicular to the long axis of the isomer, respectively. The rest of the information is the same as given in the caption for Table A.17.

Peak	$E$ (eV)	$f_{12}$	$\langle S^2 \rangle$	Wavefunction
Reference				$ H_{1\alpha}^1; H_{2\alpha}^1; H_{3\alpha}^1\rangle$
I <sub>  </sub>	2.36	0.6487	3.98	$ H_\alpha - 1 \rightarrow L_\alpha + 2\rangle(0.6487)$ $ H_\beta - 1 \rightarrow L_\beta + 2\rangle(0.5646)$
II <sub>  ,⊥</sub>	3.90	0.3729	4.00	$ H_{3\alpha} \rightarrow L_\alpha + 1\rangle(0.6329)$ $ H_\beta \rightarrow L_\beta + 1\rangle(0.4181)$
III <sub>  </sub>	4.34	0.7430	3.79	$ H_{2\alpha} \rightarrow L_\alpha\rangle(0.6197)$ $ H_{1\alpha} \rightarrow L_\alpha + 1\rangle(0.6053)$
III <sub>  </sub>	5.92	0.1573	3.91	$ H_\beta - 2 \rightarrow L_\beta\rangle(0.3742)$ $ H_\alpha - 2 \rightarrow L_\alpha\rangle(0.3477)$

**Table A.19.** Excitation energies,  $E$ , and many-particle wavefunctions of excited states corresponding to the peaks in the CIS linear absorption spectrum of B<sub>6</sub><sup>+</sup>-tetragonal bipyramid isomer (cf. Fig. 21). The subscripts || and ⊥, in the peak number denote the absorption due to light polarized in, and perpendicular to the square plane of bipyramid, respectively. The rest of the information is the same as given in the caption for Table A.14.

Peak	$E$ (eV)	$f_{12}$	$\langle S^2 \rangle$	Wavefunction
Reference				$ H_{1\alpha}^1\rangle$
I <sub>⊥</sub>	1.23	0.1144	1.29	$ H_{1\alpha} \rightarrow L_\alpha\rangle(0.9530)$ $ H_{1\alpha} \rightarrow L_\alpha + 1\rangle(0.9530)$ $ H_\beta \rightarrow L_\beta + 3\rangle(0.1202)$
II <sub>  </sub>	2.55	0.0191	2.40	$ H_\alpha - 4 \rightarrow L_\alpha\rangle(0.6498)$ $ H_\alpha - 3 \rightarrow L_\alpha + 1\rangle(0.6498)$ $ H_\beta \rightarrow L_\beta + 1\rangle(0.2971)$
III <sub>  ,⊥</sub>	3.61	0.1002	2.10	$ H_\beta \rightarrow L_\beta + 1\rangle(0.8844)$ $ H_\alpha - 4 \rightarrow L_\alpha\rangle(0.2133)$ $ H_\alpha - 3 \rightarrow L_\alpha + 1\rangle(0.2133)$
IV <sub>  </sub>	5.54	0.0223	1.36	$ H_{1\alpha} \rightarrow L_\alpha + 5\rangle(0.8524)$ $ H_\beta - 3 \rightarrow L_\beta + 3\rangle(0.2325)$ $ H_\beta - 2 \rightarrow L_\beta + 4\rangle(0.2325)$

**Table A.20.** Excitation energies,  $E$ , and many-particle wavefunctions of excited states corresponding to the peaks in the CIS linear absorption spectrum of  $B_6^+$ -linear (quartet) isomer (cf. Fig. 22). The subscripts  $\parallel$  and  $\perp$ , in the peak number denote the absorption due to light polarized along, and perpendicular to the long axis of the isomer, respectively. The rest of the information is the same as given in the caption for Table A.17.

Peak	$E$ (eV)	$f_{12}$	$\langle S^2 \rangle$	Wavefunction
Reference				$ H_{1\alpha}^1; H_{2\alpha}^1; H_{3\alpha}^1\rangle$
I $\parallel$	4.25	2.9960	5.43	$ H_\beta - 1 \rightarrow L_\beta + 1\rangle(0.5588)$ $ H_\beta \rightarrow L_\beta\rangle(0.5588)$ $ H_\alpha - 4 \rightarrow L_\alpha\rangle(0.3565)$
II $\perp$	4.66	1.1384	5.62	$ H_\alpha - 4 \rightarrow L_\alpha\rangle(0.5669)$ $ H_{1\alpha} \rightarrow L_\alpha + 2\rangle(0.4295)$ $ H_{2\alpha} \rightarrow L_\alpha + 1\rangle(0.4295)$

**Table A.21.** Excitation energies,  $E$ , and many-particle wavefunctions of excited states corresponding to the peaks in the CIS linear absorption spectrum of  $B_6^+$ -planar trimers isomer (cf. Fig. 23). The subscripts  $\parallel$  and  $\perp$ , in the peak number denote the absorption due to light polarized in, and perpendicular to the plane of the isomer, respectively. The rest of the information is the same as given in the caption for Table A.14.

Peak	$E$ (eV)	$f_{12}$	$\langle S^2 \rangle$	Wavefunction
Reference				$ H_{1\alpha}^1\rangle$
I $\parallel$	1.40	0.1363	1.17	$ H_\beta \rightarrow L_\beta\rangle(0.8954)$ $ H_\beta - 2 \rightarrow L_\beta + 1\rangle(0.2557)$
II $\perp$	2.36	0.0293	1.03	$ H_\alpha - 2 \rightarrow L_\alpha\rangle(0.6214)$ $ H_\alpha - 4 \rightarrow L_\alpha + 1\rangle(0.4845)$
III $\perp$	3.66	0.0507	1.03	$ H_\alpha - 2 \rightarrow L_\alpha + 2\rangle(0.5121)$ $ H_\beta - 1 \rightarrow L_\beta + 1\rangle(0.3618)$
IV $\perp$	4.74	0.0891	1.26	$ H_{1\alpha} \rightarrow L_\alpha + 6\rangle(0.4977)$ $ H_\alpha - 1 \rightarrow L_\alpha + 5\rangle(0.4270)$
V $\parallel$	5.19	0.1498	1.09	$ H_\alpha - 3 \rightarrow L_\alpha + 2\rangle(0.6496)$ $ H_{1\alpha} \rightarrow L_\alpha + 4\rangle(0.4993)$

## References

- J.A. Alonso, *Structure and Properties of Atomic Nanostructures* (Imperial College Press, London, 2005)
- Physics and Chemistry of Small Clusters*, edited by P. Jena, S. Khanna, B. Rao, (Plenum Publishing, New York, 1987)
- R.N. Grimes, *J. Chem. Educ.* **81**, 657 (2004)
- B. Kiran, S. Bulusu, H.J. Zhai, S. Yoo, X.C. Zeng, L.S. Wang, *Proc. Natl. Acad. Sci. USA* **102**, 961 (2005)
- C. Romanescu, T.R. Galeev, W.L. Li, A.I. Boldyrev, L.S. Wang, *Angew. Chem. Int. Ed.* **50**, 9334 (2011)
- H.J. Zhai, A.N. Alexandrova, K.A. Birch, A.I. Boldyrev, L.S. Wang, *Angew. Chem. Int. Ed.* **42**, 6004 (2003)
- I. Cabria, M.J. López, J.A. Alonso, *Nanotechnology* **17**, 778 (2006)
- H.J. Zhai, B. Kiran, J. Li, L.S. Wang, *Nat. Mater.* **2**, 827 (2003)
- J. Jimenez-Halla, R. Islas, T. Heine, G. Merino, *Angew. Chem. Int. Ed.* **49**, 5668 (2010)
- W. Huang, A.P. Sergeeva, H.J. Zhai, B.B. Averkiev, L.S. Wang, A.I. Boldyrev, *Nat. Chem.* **2**, 202 (2010)
- A.N. Alexandrova, A.I. Boldyrev, H.J. Zhai, L.S. Wang, *Coord. Chem. Rev.* **250**, 2811 (2006)
- A.N. Alexandrova, H.J. Zhai, L.S. Wang, A.I. Boldyrev, *Inorg. Chem.* **43**, 3552 (2004)
- A.N. Alexandrova, A.I. Boldyrev, H.J. Zhai, L.S. Wang, E. Steiner, P.W. Fowler, *J. Phys. Chem. A* **107**, 1359 (2003)
- S.J.L. Placa, P.A. Roland, J.J. Wynne, *Chem. Phys. Lett.* **190**, 163 (1992)
- L. Hanley, J.L. Whitten, S.L. Anderson, *J. Phys. Chem.* **92**, 5803 (1988)
- I. Boustani, *Phys. Rev. B* **55**, 16426 (1997)
- M. Atiş, C. Özdoğan, Z.B. Güvenc, *Int. J. Quantum Chem.* **107**, 729 (2007)
- S. Botti, A. Castro, N.N. Lathiotakis, X. Andrade, M.A.L. Marques, *Phys. Chem. Chem. Phys.* **11**, 4523 (2009)
- R. Shinde, A. Shukla, *Nano LIFE* **2**, 1240004 (2012)
- A. Dreuw, M. Head-Gordon, *Chem. Rev.* **105**, 4009 (2005)
- S. Tirapattur, M. Bellette, M. Leclerc, G. Durocher, *J. Mol. Struct. Theor.* **625**, 141 (2003)
- J.B. Lagowski, *J. Mol. Struct. Theor.* **589-590**, 125 (2002)
- T.A. Dahlseid, M.M. Kappes, J.A. Pople, M.A. Ratner, *J. Chem. Phys.* **96**, 4924 (1992)
- J. Cornil, D. Beljonne, R. Friend, J. Brédas, *Chem. Phys. Lett.* **223**, 82 (1994)
- L. Mitás, J. Therrien, R. Twisten, G. Belomoin, M.H. Nayfeh, *Appl. Phys. Lett.* **78**, 1918 (2001)
- K. Harigaya, S. Abe, *Phys. Rev. B* **49**, 16746 (1994)
- V. Bonačić-Koutecký, J. Gaus, M.F. Guest, J. Koutecký, *J. Chem. Phys.* **96**, 4934 (1992)
- I. Shavitt, R. Bartlett, *Many-Body Methods in Chemistry and Physics: MBPT and Coupled-Cluster Theory* (Cambridge University Press, London, 2009)
- M.J. Frisch et al., *Gaussian 09 Revision A.02* (Gaussian Inc., Wallingford CT, 2009)
- M. Kallay, J. Gauss, *J. Chem. Phys.* **121**, 9257 (2004)
- A.I. Krylov, *Ann. Rev. Phys. Chem.* **59**, 433 (2008)
- A. Allouche, *J. Comput. Chem.* **32**, 174 (2011)
- G. Wei, Z. Pu, R. Zou, G. Li, Q. Luo, *Sci. China Chem.* **53**, 202 (2010)
- V. Bonačić-Koutecký, P. Fantucci, J. Koutecký, *Chem. Rev.* **91**, 1035 (1991)
- J. Blanc, V.B. Koutecký, M. Broyer, J. Chevalyere, P. Dugourd, J. Koutecký, C. Scheuch, J.P. Wolf, L. Wöste, *J. Chem. Phys.* **96**, 1793 (1992)
- J. Ma, Z. Li, K. Fan, M. Zhou, *Chem. Phys. Lett.* **372**, 708 (2003)
- R. Shinde, A. Shukla, in preparation